SPECIES AND DEVELOPMENTAL DIFFERENCES IN MAMMALIAN RESPIRATORY RHYTHM GENERATION

by

BARBARA MARIE GAJDA

B.Sc.H., The University of Winnipeg, 2004

A THESIS SUBMITTED IN PARTIAL FULFILLMENT OF
THE REQUIREMENTS FOR THE DEGREE OF

MASTER OF SCIENCE

in

THE FACULTY OF GRADUATE STUDIES

(Zoology)

THE UNIVERSITY OF BRITISH COLUMBIA

September 2007

© Barbara Marie Gajda, 2007

Abstract

Mammalian neonates can recover spontaneously from hypothermia-induced respiratory arrest when re-warmed (termed autoresuscitation). As a rat ages, autoresuscitation ability is lost during a transitional period ('developmental window') between 16 - 20 post-natal days (PND) so that hypothermic respiratory arrest results in death for a mature rat. Hamsters retain the ability to autoresuscitate past this developmental window. The retention of this ability in hamsters implies that there may be fundamental differences in the central rhythm generator (CRG) of rats and hamsters. This study tests the hypothesis that the contribution to respiratory rhythm generation of the putatively rhythmogenic persistent Na^+ current (I_{NaP}) and Ca^{2+}-activated non-selective cation current (I_{CAN}), two currents which may facilitate the initiation of breathing after arrest, is different between rats and hamsters. Because autoresuscitation ability is lost during development, we also test the hypothesis that the I_{NaP} and I_{CAN} contribution to respiratory rhythm generation change as a rat ages.

We applied riluzole (I_{NaP} blocker) and flufenamic acid (FFA; I_{CAN} blocker) to the arterially perfused *in situ* working heart-brainstem preparation in hamsters and two age groups of rats (12 - 14 PND, >23 PND). Application of riluzole and FFA to rats and hamsters showed that elimination of I_{NaP} and I_{CAN} resulted in profound decrease in phrenic burst frequency in hamsters with little change in rats. This result is consistent with the hypothesis that a phylogenetic difference exists in the mechanism of setting respiratory rhythm in the CRG of rats and hamsters. Comparisons between young and weaned rats showed that young rats tended to be more sensitive to the application of riluzole and FFA than weaned rats. The small differences observed between young and weaned rats in the reliance on I_{NaP} and I_{CAN} for respiratory rhythm generation are consistent with the hypothesis that a developmental change occurs in the CRG of rats during maturation. Increasing the proportion of CO_2 that the preparations were exposed to increased neural ventilation in weaned rats suggesting that I_{NaP} and I_{CAN} provide a source of excitatory drive to the CRG.

Table of contents

List of tables

List of figures

List of abbreviations

BötC	Bötzinger Complex
CRG	Central rhythm generator
CVN	Cervical vagus nerve
cVRG	Caudal ventral respiratory group
FFA	Flufenamic acid
I_{CAN}	Ca^{2+}-activated non-selective cation current
I_{K+LEAK}	K^+ leak current
I_{NaP}	Persistent Na^+ current
I_{NaT}	Transient Na^+ current
mV	Millivolts
$n\dot{V}_E$	Neural ventilation
pA/pF	Unit for current density (picoamperes/picoFarads)
PBC	preBötzinger Complex
PND	Post-natal days
RIL	Riluzole
rVRG	Rostral ventral respiratory group
T_E	Expiratory duration or interburst interval
T_I	Inspiratory duration
V_M	Membrane potential
VRG	Ventral respiratory group
XII	Hypoglossal nerve

Acknowledgements

This research project would not have been completed if not for the technical expertise and friendship of Angelina Fong who originally taught the working heart-brainstem preparation to me in Missouri and after continued to be a source of advice and encouragement with respect to the many downs and ups the WHBP as well as the experimental design of this project.

I would like to also acknowledge my supervisor, Bill Milsom, for his expertise and support and for deliberately creating a familial environment in our lab. Thank you to my committee members Vanessa Auld and Matt Ramer for their helpful feedback on experimental design, data analysis and thesis drafts. Thank you also to Jeffrey T. Potts at the University of Missouri-Columbia for hosting me in his lab for two weeks in February 2005 while I learned the WHBP and for loaning me a pump that I have yet to return.

I would like to thank Bruce Gillespie, Vince Grant, and Don Brandys in the mechanical and electrical shops for building and repairing many essential parts of my rig.

I would like to extend my gratitude and affection to past and present members of the Milsom lab who encouraged my academic growth as well as opportunities for fun and silliness throughout my degree. Finally, I would like to recognize my parents, Krys and Bo, brother Marek, my mentors Ted and Nancy, fellow members of Development and Peace and my friends and community at St. Mark's Chapel/St. Ignatius Parish whose prayers and encouragement have sustained me over the past three years. I especially would like to remember Fr. Brian Burns who passed away suddenly in June 2007 because of his formative impact on my life.

1. Introduction

1.1. Hypothermic respiratory arrest and autoresuscitation

When the body temperature of an animal is reduced in an uncontrolled manner (hypothermia), respiration first slows then stops (termed hypothermic respiratory arrest). Most adult mammals can withstand only a certain level and duration of hypothermia before vital processes fail irreversibly. Respiratory arrest is followed by cardiac arrest and eventually death (Tattersall & Milsom, 2003). Neonatal mammals, however, have been observed to remain in a state of respiratory arrest for up to three hours at hypothermic temperatures and fully recover (Adolph, 1951) by spontaneous resuscitation (autoresuscitation) upon gradual re-warming without the need for artificial intervention (as is necessary for adults) (Adolph, 1951; Hill, 2000). Marshall (2005, unpublished) determined that a critical period in development exists when maturing rats lose the ability to autoresuscitate. This 'developmental window' begins at 14 post-natal days (PND) and autoresuscitation ability is completely lost by 18 - 20 PND; after this window hypothermic respiratory arrest results in death in the absence of intervention (Marshall, 2005).

Hamsters, permissive hibernators, also have autoresuscitation ability; however they maintain this ability past the developmental window of rats (Marshall, 2005) and throughout adulthood (Andrade *et al.*, unpublished). Therefore, hamsters do not exhibit a developmental window as rats do.

Hypothermic respiratory arrest occurs due to the failure of the respiratory central rhythm generator (CRG) in the medulla to generate a rhythm, rather than the failure of motoneurons to propagate the signal or the loss of motor function in the respiratory muscles (Mellen *et al.*, 2002; Tattersall & Milsom, 2003). Therefore, a difference may exist in the CRG between species that maintain autoresuscitation ability (hamsters) compared to species that do not (rats).

1.1.1. Background information on respiratory rhythm generation

The motion of breathing is comprised of two mechanical movements: inspiration and expiration. However from the perspective of neurobiology, breathing is comprised of three neural phases: inspiratory, post-inspiratory and expiratory phases. The post-inspiratory phase, arising between the antagonistic inspiratory and expiratory phases of muscle activity, is associated with

passive expiration and constriction of upper airway muscles (Richter, 1982). Respiratory neurons responsible for generating respiratory rhythm are classified according to the neural phase in which the neurons display activity and are found within a large heterogeneous group of respiratory neurons in the ventrolateral medulla known as the ventral respiratory group (VRG) (Figure 1-1). The VRG extends from the first cervical segment (C1) rostrally to abut the facial nucleus (Ellenberger & Feldman, 1990). It can be subdivided rostrocaudally into 4 divisions: the Bötzinger Complex (BötC), the preBötzinger Complex (PBC), the rostral VRG (rVRG) and the caudal VRG (cVRG).

The PBC has been postulated to be the site of inspiratory rhythm generation in the brainstem. The PBC can be isolated chemically or physically from the rest of the respiratory column *in vitro* and will continue to generate respiratory-like rhythm (Smith *et al.*, 1991)(Johnson *et al.*, 2001). Several ablation studies in intact animals (rats and goats) have shown that destroying PBC neurons will severely disrupt breathing (Wenninger *et al.*, 2004)(Gray *et al.*, 2001)(McKay *et al.*, 2005), supporting the hypothesis that the PBC is vital for respiratory rhythm generation.

Because respiratory rhythm can be maintained when inhibitory synaptic connections are blocked, inspiratory neurons with intrinsic bursting (pacemaker) ability expressing a voltage-dependent persistent sodium current (I_{NaP}) were proposed to be necessary to set respiratory rhythm (Smith *et al.*, 1991; Johnson *et al.*, 1994; Del Negro *et al.*, 2002a; Del Negro *et al.*, 2002b). I_{NaP} is active at more negative membrane potentials than other currents: I_{NaP} is active between -60 and -40 mV, transient sodium current (I_{NaT}) is active at -34 mV (Richter & Spyer, 2001)(Butera Jr. *et al.*, 1999)(Urbani & Belluzzi, 2000)(Alzheimer *et al.*, 1993). I_{NaP} is found in several neural tissues (such as the rostral ventrolateral medulla, spinal cord, petrosal ganglion, suprachiasmatic nucleus, neocortex) (Rybak *et al.*, 2003)(Urbani & Belluzzi, 2000; Darbon *et al.*, 2004; Kononenko *et al.*, 2004; Faustino & Donnelly, 2006) and is expressed in all respiratory neurons in the rVRG, however at a greater current density (pA/pF) in PBC interneurons (Ptak *et al.*, 2005).

I_{NaP} facilitates respiratory rhythm generation by promoting plateau potentials and repetitive firing and by increasing neuron excitability (as depicted in Figure 1-2). I_{NaP} is activated at -60 mV and depolarizes the membrane to the activation threshold for I_{NaT} (Figure 1-2B③),

leading to voltage-dependent bursting (Figure 1-2B①) (Feldman & Del Negro, 2006). During the action potential I_{NaT} becomes inactivated rapidly; however, due to the slow inactivation of I_{NaP}, the membrane potential remains elevated allowing repetitive bursting (Figure 1-2B) to continue until I_{NaP} is eventually inactivated (Figure 1-2B②) (Crill, 1996)(Del Negro *et al.*, 2002b)(Feldman & Del Negro, 2006). By not rapidly inactivating following an action potential, I_{NaP} prevents the afterhyperpolarization that follows every spike thereby promoting another burst in the spike train (Figure 1-2A②) (Lee & Heckman, 2001).

I_{NaP} is expressed ubiquitously in the PBC; however not all PBC neurons have bursting pacemaker properties even though I_{NaP} appears to perform similar functions in non-pacemaker and pacemaker neurons. Therefore, bursting pacemaker neurons are characterized not just by the presence of I_{NaP} but by a ratio of I_{NaP} to K^+ leak currents (I_{K+LEAK}) and by the ability to continue firing when synaptically isolated (Del Negro *et al.*, 2002b; Ptak *et al.*, 2005). I_{NaP} confers bursting properties and increases the excitability of all respiratory neurons (pacemaker and non-pacemaker). However, by interacting with I_{K+LEAK}, I_{NaP} may have a more specific role in setting inspiratory rhythm in bursting pacemaker neurons with intrinsic rhythmicity by increasing the rate of membrane depolarization to threshold levels for action potential generation (-40 mV) (Figure 1-2B①) (Del Negro *et al.*, 2002b).

Another current thought to bestow bursting pacemaker properties to another set of inspiratory neurons within the PBC is the calcium-activated non-selective cation current, I_{CAN} (Thoby-Brisson & Ramirez, 2001; Pena *et al.*, 2004). I_{CAN} is found in many regions of the brain and body (Gogelein *et al.*, 1990; Hall & Delaney, 2002)(Cho *et al.*, 2003) including the VRG (Pena *et al.*, 2004; Del Negro *et al.*, 2005). I_{CAN} is expressed in nearly all PBC neurons; its mechanism is voltage-independent but requires increased cytoplasmic Ca^{2+} in order to be activated (Del Negro *et al.*, 2005)(Hall & Delaney, 2002). Upon activation by increased intracellular Ca^{2+}, I_{CAN} produces a depolarizing current (Partridge *et al.*, 1994). Since the I_{CAN} channels do not rapidly inactivate, I_{CAN} contributes to bursting and plateau potentials also (Partridge *et al.*, 1994)(Hall & Delaney, 2002)(Rekling & Feldman, 1997). Recent evidence also has suggested that I_{CAN} contributes to the inspiratory drive potential which is a 10 - 30 mV depolarization of the

membrane that brings the neuron to threshold potential for bursting (Figure 1-2A) thereby increasing the excitability of respiratory neurons (Pace *et al.*, 2007a).

Thus, both I_{NaP} and I_{CAN} are involved in generating respiratory output by promoting bursting, producing plateau potentials and increasing neuronal excitability. Their proposed role in setting respiratory rhythm is derived from the observation of respiratory neurons in the PBC that continue bursting when synaptically isolated (Thoby-Brisson & Ramirez, 2001; Pena *et al.*, 2004). These neurons have been presumed to be rhythmogenic because of their intrinsic bursting ability (conferred by I_{NaP} or I_{CAN}) and are proposed to compose a kernel of respiratory neurons, embedded in a network of reciprocally inhibited respiratory neurons, that sets the baseline rhythm for the respiratory network and eventually produces rhythmic motor output (Smith *et al.*, 2000).

Riluzole, a neuroprotective and antiepileptic drug, blocks I_{NaP} and has been widely used to assess the importance of I_{NaP} to respiratory rhythm generation (Thoby-Brisson & Ramirez, 2001; Del Negro *et al.*, 2002a; Abdala *et al.*, 2004; Pena *et al.*, 2004; Smith *et al.*, 2004). At appropriate concentrations (EC_{50} = 2 - 3 μM), riluzole has been shown to be effective in selectively blocking the I_{NaP} in brainstem transverse slice and isolated brainstem-spinal cord (en bloc) preparations (Urbani & Belluzzi, 2000)(Del Negro *et al.*, 2005). Flufenamic acid (FFA), a non-steroidal anti-inflammatory drug, blocks the I_{CAN} current when applied at 100 - 500 μM in brainstem transverse slice preparations (Gogelein *et al.*, 1990; Pena *et al.*, 2004; Del Negro *et al.*, 2005)(Cho *et al.*, 2003)(Pace *et al.*, 2007a)(Pace *et al.*, 2007b). Both drugs are commonly used in studying the contribution of I_{NaP} and I_{CAN} to respiratory rhythm generation.

1.2. Phylogeny and respiratory rhythm generation

1.2.1. Do phylogenetic differences exist in the roles of I_{NaP} and I_{CAN} in respiratory rhythm generation?

Hypothermic respiratory arrest and recovery from arrest originates at the respiratory CRG in the medulla (Mellen *et al.*, 2002; Tattersall & Milsom, 2003). Therefore, the ability of adult hamsters and the inability of adult rats to restart breathing after hypothermic respiratory arrest may reflect a fundamental difference in the mechanism of respiratory rhythm generation in these

two species. Since I_{NaP} and I_{CAN} facilitate inspiratory burst generation, they may be important in the recovery from hypothermic respiratory arrest by providing drive to the CRG to initiate breathing. Because adult hamsters are able to recover from respiratory arrest, we hypothesize that hamsters have a greater dependence on I_{NaP} and I_{CAN} for respiratory rhythm generation than rats.

1.3. Ontogeny and respiratory rhythm generation

In rats, a developmental window exists where the ability to recover from hypothermic respiratory arrest is lost as the rat ages (Marshall, 2005). This loss of autoresuscitation ability implies that there are changes occurring in the CRG with development. We hypothesize that I_{NaP} and I_{CAN} are involved with initiating breathing after arrest and therefore asked if the reliance on I_{NaP} and I_{CAN} for rhythm generation changes during development. Several maturational changes occur in the PBC in the first 12 days after birth: increased expression of excitatory neurotransmitters as well as a reversal of $GABA_A$ receptor-mediated modulation (Wong-Riley & Liu, 2005)(Liu & Wong-Riley, 2004). The switch in the expression of $GABA_A$ receptor subunits at 12 PND results in a change in the GABA signal (via $GABA_A$) from depolarizing to hyperpolarizing (Liu & Wong-Riley, 2004). [This GABAergic switch is distinct from the Cl^- current reversal which occurs at about embryonic day 19 due to increased Cl^- ion extrusion by the KCC2 cotransporter (Ren & Greer, 2006).] The membrane potential of respiratory neurons hyperpolarizes (to <-65 mV) over development so that I_{NaP} is not active until the membrane is depolarized to -60 mV (Richter & Spyer, 2001). The switch from GABAergic depolarization to hyperpolarization at 12 PND may contribute to the further hyperpolarizing of membrane potential of respiratory neurons in the PBC (Wong-Riley & Liu, 2005)(Liu & Wong-Riley, 2004). Inhibitory synaptic inputs act as a functional synaptic voltage clamp to hold the membrane of rhythmogenic neurons at voltages where I_{NaP} and I_{CAN} are not active (Richter & Spyer, 2001). It is unknown how these changes might affect the generation of respiratory rhythm of the developing mammal.

1.3.1. Do ontogenetic differences exist in the roles of I_{NaP} and I_{CAN} in respiratory rhythm generation?

While most of the current literature examines the role of I_{NaP} and I_{CAN} in early post-natal development (Pena *et al.*, 2004; Del Negro *et al.*, 2005; Pace *et al.*, 2007b; Pena & Aguileta, 2007), results from our laboratory suggest that the role of I_{NaP} in rhythm generation may be changing as

rats mature (Marshall, 2005). The proportion of I_{NaP} and I_{CAN}-mediated bursting pacemaker neurons in the PBC increase up to 15 PND (Pena *et al.*, 2004; Del Negro *et al.*, 2005); however, the increase in $GABA_A$-mediated inhibition in the PBC should counter the role of I_{NaP} and I_{CAN} in the expression of respiratory rhythm beyond 12 PND (Liu & Wong-Riley, 2004). Because rats lose the ability to autoresuscitate during development, a change may be occurring during development in the contribution of I_{NaP} and I_{CAN} to maintaining normal respiratory rhythm.

We hypothesize that during development changes are occurring in the CRG, particularly in the currents that engender intrinsic bursting (I_{NaP} and I_{CAN}), that cause the neonate to 'out-grow' the ability to autoresuscitate. We hypothesize that the influence of I_{NaP} and I_{CAN} on rhythm generation declines so that adult mammals depend less on I_{NaP} and I_{CAN} than neonatal mammals for rhythm generation.

To test our hypotheses that phylogenetic and ontogenetic differences occur in the roles of I_{NaP} and I_{CAN}, we eliminated I_{NaP} and I_{CAN} in the arterially perfused *in situ* working heart-brainstem preparation and examine the effect of the elimination of these currents on respiratory rhythm generation. Because both hamsters and young rats are capable of autoresuscitation, which may imply a greater dependence on I_{NaP} and I_{CAN} for rhythm generation, we expect that the elimination of these currents will result in a greater decrease in respiratory output in mature hamsters and young rats than in mature rats.

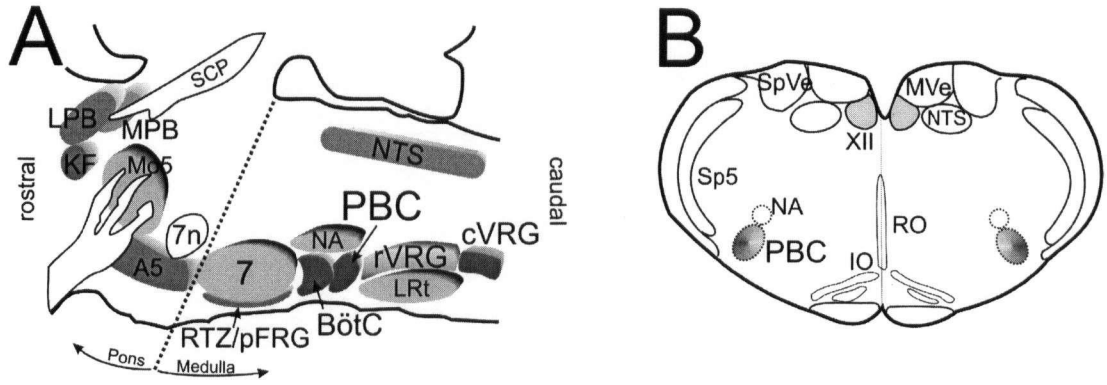

Figure 1-1: Respiratory column location in the brainstem of mammals.
Parasagittal (A) and transverse (B) views of brainstem adapted from Alheid et al. (2004) and Richter and Spyer (2001). Dashed line (A) delineates the pons from medulla. Abbreviations: 7, facial nucleus; 7n, facial nerve; A5, pontine noradrenergic group; BötC, Bötzinger Complex; cVRG, caudal ventral respiratory group; IO, inferior olive; KF, Kölliker-Fuse nuclei; LPB, laternal parabrachial nucleus; LRt, lateral reticulum; MPB, medial parabrachial nucleus; MVe, medial vestibular nucleus; Mo5, trigeminal motor nucleus; NA, nucleus ambiguus compactum; NTS, nucleus of the solitary tract; PBC, preBötzinger Complex; RO, nucleus raphe obscurus; RTZ/pFRG, region of the retrotrapezoid nucleus and parafacial respiratory group; rVRG, rostral ventral respiratory group; SCP, superior cerebellar peduncle; Sp5, spinal trigeminal nucleus; SpVe, spinal vestibular nucleus.

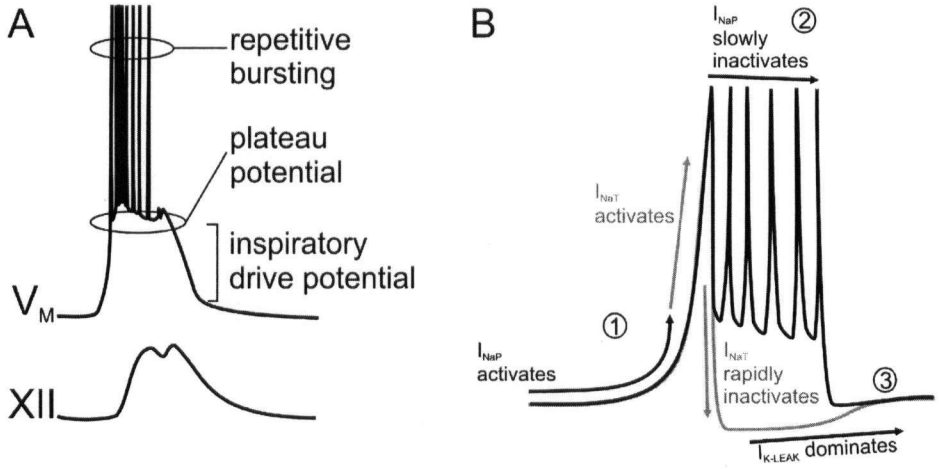

Figure 1-2: Bursting in respiratory neurons.
(A) Simplified example of patch recording of the membrane potential (V_M) of a bursting inspiratory cell and rectified, integrated motor output from hypoglossal nerve (XII). Example redrawn from Pace et al. (2007). (B) I_{NaP}-mediated pacemaker neuron bursting is represented in black. Grey line predicts action potential trajectory in the absence of I_{NaP}. Please see text for description.

2. Methods

Experimental protocols were approved by the Animal Care Committee of the University of British Columbia acting under the guidelines set by the Canadian Council for Animal Care (CCAC).

2.1. In situ working heart-brainstem preparation

We used the *in situ* arterially perfused working heart-brainstem preparation (subsequently referred to as the *in situ* preparation) (Paton, 1996) as depicted in Figure 2-1. In brief, a Sprague-Dawley rat (*Rattus norvegicus*; UBC Rodent Breeding facilities) or hamster (*Mesocricetus auratus*; Charles River, Wilmington, MA) was anaesthetised deeply by halothane or isofluorane. The animal was transected caudal to the diaphragm and the anterior portion of the body was placed in chilled modified Ringer's solution (approximately 4 - 10 °C) bubbled with 95% O_2/5% CO_2 carbogen gas. The dorsal braincase was removed and the animal was decerebrated at the precollicular level as indicated in Figure 2-2. The skin and any remaining abdominal viscera were removed and the diaphragm was removed carefully from the dorsal body wall and peeled back to expose the thoracic cavity. The descending aorta was separated from the dorsal body wall before the body wall was removed. The lungs were removed and the left phrenic nerve and pericardial cavity were cleared of any connective tissue. In a number of preparations, the right cervical vagus nerve (CVN) also was isolated by separating the nerve from the carotid artery in the neck and cutting the nerve at the most caudal point in the neck.

The dissected preparation then was transferred to an acrylic recording chamber, placed dorsal side up, and secured at the head with ear bars. A double lumen catheter was inserted into the descending aorta to begin flow of perfusate to the preparation. Pump flow was calibrated prior to the experiments and flow rates for the groups are recorded in Table 2-1. The perfusate (modified Ringer's + 1.25% Ficoll® PM 70) was aerated with carbogen gas and warmed to 31 - 32°C by a heat exchanger then passed through bubble traps and a Millipore filter (25 μM) before entering the preparation. Upon warming of the preparation, the heart resumed beating, followed by inspiratory contractions of the diaphragm and intercostal muscles. The preparation was paralysed by adding a neuromuscular junction blocker, either rocuronium bromide (Zemuron, 2 mg) or vecuronium bromide (Norcuron, 0.6 mg), directly to the perfusate.

The left phrenic nerve was snipped at the diaphragm and both the cervical vagus and phrenic nerve (PHR) were connected to bipolar suction electrodes. The signals measured by the suction electrodes were passed through pre-amplifiers (FRAMP PRA-1,-2) then amplified (200 x) and filtered (500 Hz - 1kHz, FRAMP GPA-1). Perfusion pressure was measured by one lumen in the catheter connected to a physiological pressure transducer (Narco Scientific) connected to an amplifier (Gould Universal). Amplified nerve signals and perfusion pressure were sampled at 2.0 kHz and recorded by Windaq data acquisition software (DataQ Instruments, Akron, OH, USA).

2.2. Experimental protocol

Only male rats and Syrian (also known as golden) hamsters were used. Rats lose autoresuscitation ability between 16 - 18 PND (Marshall, 2005), so ages were chosen on either side of this developmental window. Rats were grouped as young rats (12 - 14 PND) or weaned rats (24 - 30 PND). The developmental stage of hamsters was matched to weaned rats (Clancy *et al.*, 2001); weaned hamsters used were 23 - 40 PND. Table 2-2 contains the mean weights of the different age groups.

All age groups underwent the same protocol. The preparation was allowed to stabilize for 30 - 60 minutes before drugs were applied incrementally. Figure 2-3 shows a representative trace of CVN and PHR discharge activity measured at the beginning of an experiment using young rat and hamster preparations to validate the viability and stability of these preparations. Stable and viable preparations are characterised by an incrementing PHR discharge and observable three-phase respiratory discharge from the CVN (Paton, 1996). As CVN discharge was used only for validation, it was not quantified.

The drug regimen involved applying riluzole and FFA individually and in combination. When riluzole or FFA was applied individually, thirteen concentrations were administered, ranging 0.2 - 20 μM for riluzole and 0.25 - 25 μM for FFA. Because other authors have used larger concentrations of FFA in brainstem transverse slice preparations to completely eliminate I_{CAN} (Del Negro *et al.*, 2005; Pace *et al.*, 2007a), a small number of experiments were run in which concentrations of 25 - 100 μM FFA were applied only to weaned rat preparations in order to see if increasing FFA would result in a change in respiratory motor output. When riluzole and FFA were coapplied, only six concentrations were applied that had been calculated to result in a 5, 10,

15, 20, 25 or 50% decrease in frequency and amplitude from baseline values when the drug was applied individually (without correcting for vehicle controls). In all cases, sufficient time after each drug application was given in order for the response to stabilize (approximately 5 - 15 minutes depending on flow rate).

Del Negro and colleagues (2005) showed that riluzole and FFA were effective in abolishing respiratory rhythm in *in vitro* transverse brainstem slice preparations. Application of substance P (excitatory neurotransmitter) rescued respiratory rhythm by increasing drive in the respiratory network. In order to increase respiratory drive in the *in situ* preparation, we increased the proportion of CO_2 bubbling in the perfusate to 7% (93% O_2). In these experiments, the preparation was initially perfused and allowed to stabilize with 5% CO_2 perfusate for 30 - 60 minutes. The gas mixture was then switched to 93% O_2/7% CO_2 and the preparation was allowed to stabilize for another 20 - 30 minutes until it had reached a steady state. When the preparation had stabilized, I followed the same combined drug regimen (riluzole and FFA) as described for the preparations using 5% CO_2.

Riluzole (Sigma, St. Louis, MO; 25 mg) was solubilized with 2 ml of 1.0 M hydrochloric acid and heated while stirring until all the riluzole dissolved. The solution was diluted to a concentration of 2 mM by adding 50 ml de-ionized distilled water (ddH_2O). FFA (Sigma, St. Louis, MO) was solubilized with 100 mM NaOH and then titrated to pH 7.4 - 8.0 with 1.0 M and 0.1 M HCl. The solution was diluted to 5 mM by adding ddH_2O. For all experiments, vehicle controls, using just the solvent for each drug, were run by adding the same volume of solution that had been added in the drug runs to correct for effects of increase perfusate volume and time.

2.3. Data and statistical analysis

The data collected by Windaq was imported and analyzed in Spike2 software (v 4.24, Cambridge Electronic Designs, Cambridge, UK). Figure 2-4 shows how the variables measured were derived from the phrenic neurogram (PHR). Inspiratory duration, T_I, was measured as the time between the onset and end of phrenic bursting; expiratory duration, T_E, was measured as the time between the end of a phrenic burst and the onset the following burst. The inverse of the sum of T_I and T_E was multiplied by 60 to calculate burst frequency (bursts min^{-1}). Amplitude of the phrenic burst was also measured as the peak of the burst in the rectified integrated neurogram.

Amplitude and frequency then were multiplied for a measure of "neural ventilation" ($n\dot{V}_E$). These variables were measured for the 60 seconds of steady-state activity preceding each drug application. The values for 60 seconds were averaged and normalized to the baseline value recorded before drug applications began; therefore, changes in fictive respiration in response to increasing concentrations of riluzole or FFA are expressed as a proportion of the baseline value (baseline=1.0). These normalised values were corrected for time by dividing the experimental values by the vehicle control values. SigmaStat was used for statistical analysis.

The data were not distributed normally and an arcsine square root transformation was not possible due to the proportion values being >1.0; therefore, the data were ranked and then tested using a two-way repeated measures ANOVA with a Student-Newman-Keuls post-hoc test with $P < 0.050$ considered significant. For the experiments using high concentration of FFA on only weaned rat preparations, the data were ranked and tested using a one-way repeated measured ANOVA and Student-Newman-Keuls post-hoc test ($P < 0.050$).

Table 2-1: The range, mean and median perfusate flow rate values to *in situ* preparation.

Age group	Range (ml/min)	Mean ± SD (ml/min)	Median (ml/min)
Young rats	8 - 18	12.9 ± 2.7	12
Weaned rats	30 - 40	34.4 ± 4.3	32
Weaned hamsters	19 - 38	29.0 ± 5.3	30

Table 2-2: The range, mean and median weight values of young rats, weaned rats and weaned hamsters used in the *in situ* preparation.

Age group	Range (g)	Mean ± SD (g)	Median (g)
Young rats	20 - 41	28.1 ± 4.0	27.5
Weaned rats	68 - 107	85.7 ± 15.7	82
Weaned hamsters	33 - 100	62.9 ± 18.9	62

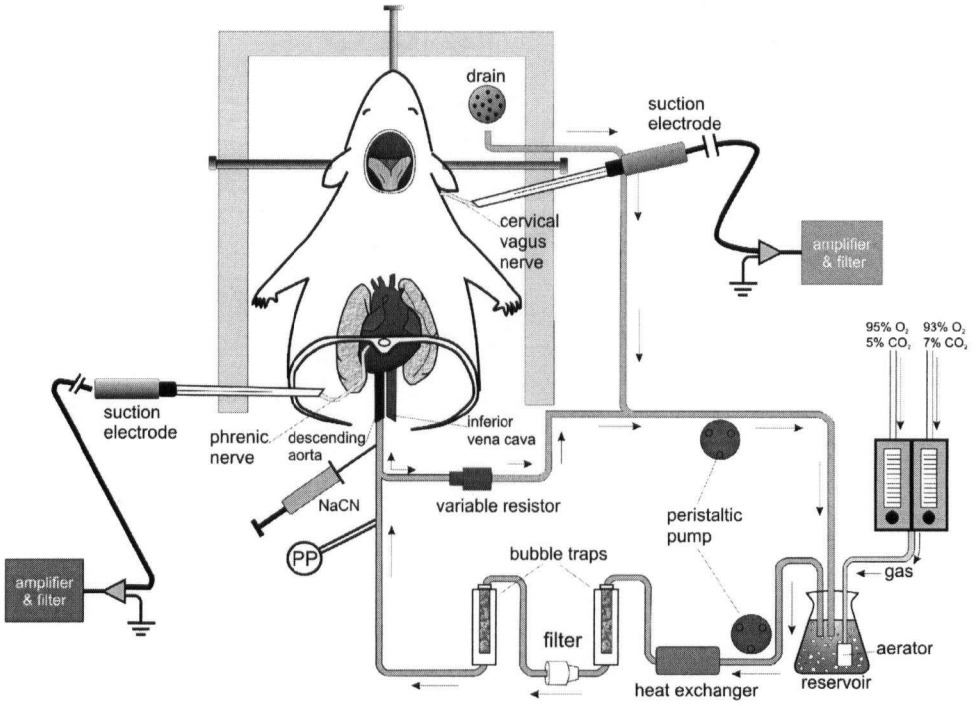

Figure 2-1: Schematic diagram of the *in situ* working heart-brainstem preparation.
The transected, decerebrated rodent is retrogradely perfused with a modified Ringer's solution containing 1.25% Ficoll that has been aerated with carbogen gas, warmed to 31 - 32 °C and filtered. Respiratory motor output is measured by recording phrenic nerve activity and cervical vagus nerve activity with suction electrode. These signals are further amplified, filtered and recorded. Schematic diagram is redrawn and adapted from Potts et al. (Potts *et al.*, 2000).

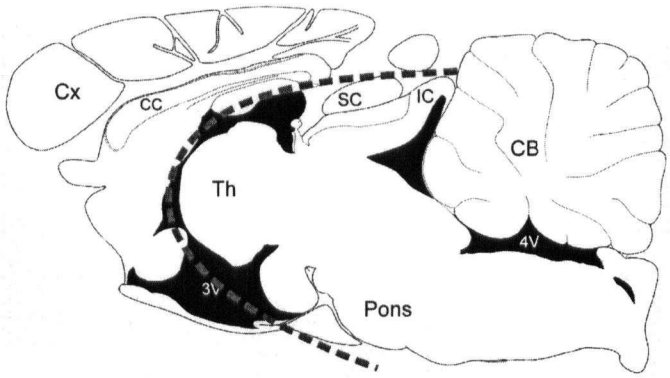

Figure 2-2: Approximate location of decerebration in a sagittal section of the rat brain.
The decerebration removes structures of the brain anterior to the thalamus and retains the areas of the thalamus, colliculi, pons, cerebellum, brainstem and spinal cord. Abbreviations: 3V, third ventricle; 4V, fourth ventricle; CB, cerebellum; CC, corpus callosum; Cx, cerebral cortex; IC, inferior colliculus; Th, thalamus; Pons, pons; SC, superior colliculus. Adapted from Paxinos and Watson (Paxinos & Watson, 1986).

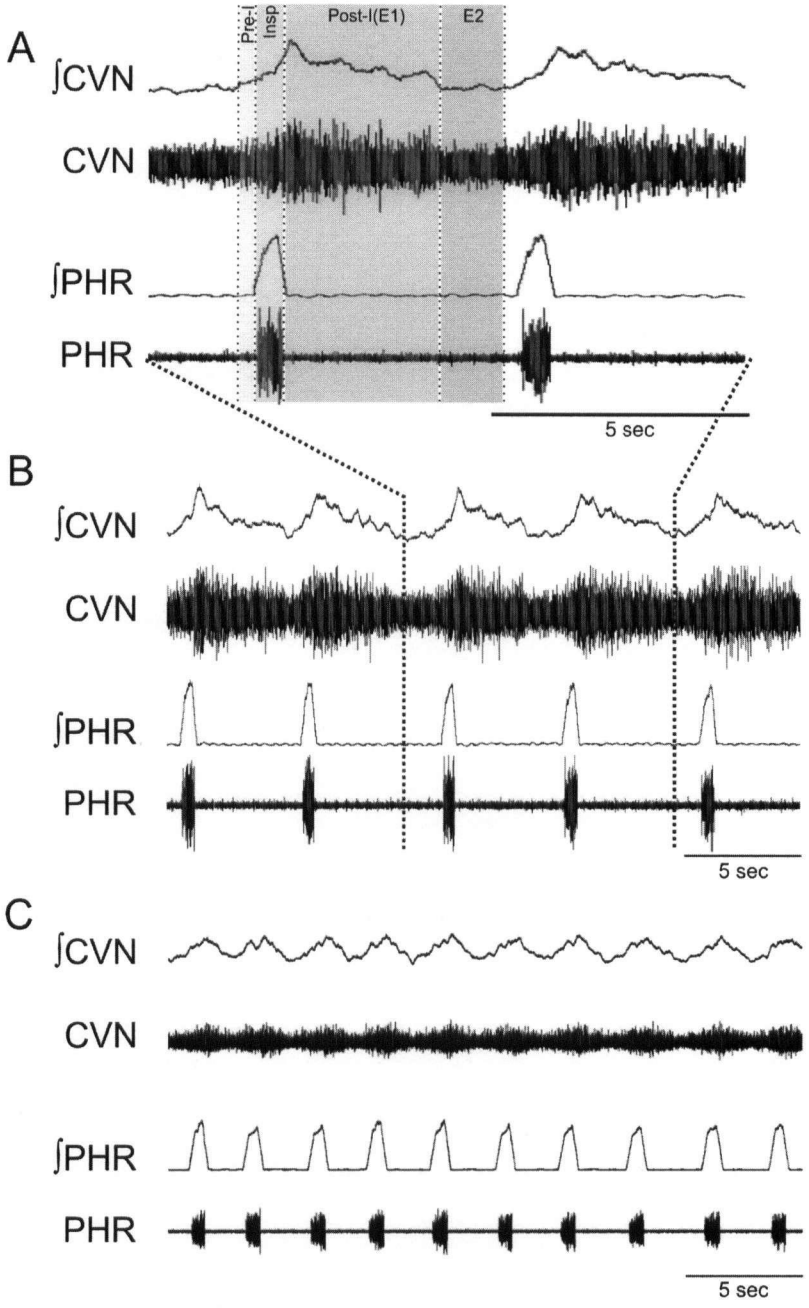

Figure 2-3: Representative neurograms of respiratory activity in young rat and hamster *in situ* preparations.
(A) Expanded view of (B) young rat and (C) hamster raw and rectified, integrated (∫) cranial vagus nerve (CVN) and phrenic nerve (PHR) neurograms measured to deduce the stability of the *in situ* preparation. Viable *in situ* preparations are characterised by CVN activity during the pre-inspiratory (Pre-I) period preceding the PHR burst, during the inspiratory (Insp) phase during the PHR burst, during the post-inspiratory (Post-I/E1) phase following the PHR burst but quiescence during the period between the Post-I and Pre-I phases, known as the expiratory phase (E2) (Paton, 1996).

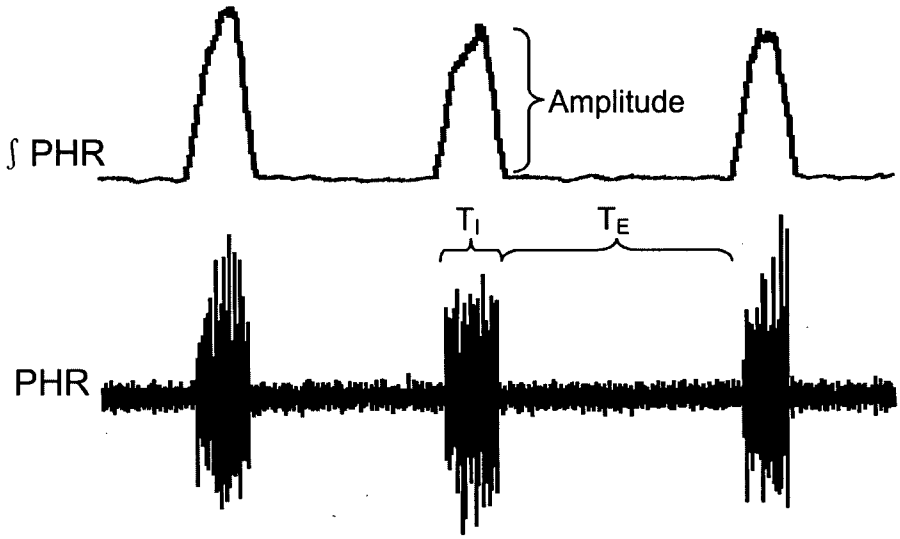

Figure 2-4: Variables measured from a phrenic neurogram.
The top trace is the rectified integrated trace of phrenic nerve activity and the bottom trace is the raw neurogram. Abbreviations: T_I, inspiratory duration; T_E, expiratory duration.

3. Results

In this study, riluzole (I_{NaP} blocker) and flufenamic acid (FFA; I_{CAN} blocker) were applied to the *in situ* preparation in young (12 - 14 PND) and weaned (23 - 30 PND) rats and weaned hamsters (>23 PND) to test the phylogenetic and ontogenetic differences in the contribution of I_{NaP} and I_{CAN} to respiratory rhythm generation. The ages of the rat groups were chosen based on a hypothesized critical developmental period between 16 - 18 PND in rats when the ability to spontaneously recover from hypothermia-induced respiratory arrest is lost (described in section 1.1). Hamster ages were chosen to match the developmental stage of the weaned rat group. Based on our hypotheses, we expected that respiratory output of the groups capable of autoresuscitation from hypothermic respiratory arrest, young rats and weaned hamsters, would decrease to a greater extent than the motor output from weaned rat preparations when I_{NaP} and I_{CAN} were eliminated.

The mean and range of starting frequency of bursts measured from the phrenic nerve for young rat, weaned rat and hamster preparations are recorded in Table 3-1. Hamster preparations tended to have much faster bursting rates than either groups of rats, but hamster preparations also had more variation in starting bursting rate.

3.1. Riluzole application

Riluzole blocks specifically I_{NaP} when applied at low concentrations. At the beginning of this study, riluzole had not been applied to the *in situ* preparation. In brainstem transverse slice preparations, concentrations of 1 - 200 μM riluzole had been applied (Del Negro *et al.*, 2002a; Pena *et al.*, 2004; Del Negro *et al.*, 2005). We began applying riluzole at 0.2 μM to 20 μM which yielded a reduction in motor output; therefore, higher concentrations were not applied.

Not all preparations continued generating respiratory motor output for all concentration of riluzole; Table 3-2 shows the number of preparations still producing phrenic motor output at the indicated concentration of riluzole. As the concentration of riluzole increased to 20 μM, only 27% of young rats continued to generate motor output. All weaned rat preparations continued generating phrenic bursts to 20 μM; however, no hamster preparation continued respiratory rhythm generation past 14 μM. Figure 3-1 shows examples of continuous tracings from the raw and rectified integrated neurogram of phrenic nerve discharge in young and weaned rats and

weaned hamster at representative concentrations. Neither the young rat nor the hamster showed continued bursting at 20 μM, but both showed profound decreases in frequency and amplitude at 8 μM where only an amplitude decrease was observed in the weaned rat.

Burst frequency, amplitude, and neural ventilation ($n\dot{V}_E$) were quantified, corrected for vehicle controls and presented as relative to baseline (= 1.0) in Figure 3-2. Frequency (Figure 3-2A) did not change significantly from baseline values (0 μM) at low concentrations for either age of rat. However, as concentration increased, frequency decreased significantly from baseline in the young rats but not in the weaned rats leading to a significant difference between the ages by 10 μM. In contrast, the frequency of phrenic bursts profoundly decreased at very low concentrations in hamster preparations. For instance, 50% of baseline frequency was reached by 1 - 2 μM riluzole in hamsters; in young rats, 10 - 12 μM riluzole was required for this degree of change. Weaned rat frequency never reached 50%. A statistically significant difference existed between hamsters and both age groups of rats at low concentrations.

Amplitude (Figure 3-2B) did not change significantly in young or weaned rat preparations at low concentrations. However, as concentration increased, the amplitude in young rat preparations declined significantly and became significantly different from the amplitude in weaned rat preparations. The amplitude of phrenic bursts decreased significantly in hamster preparations after 6 μM. Between 6 and 10 μM, hamster preparations were significantly different from both ages of rats.

Neural ventilation, $n\dot{V}_E$, (Figure 3-2C) in weaned rats did not change significantly from baseline until 18 μM. Young rats significantly decreased $n\dot{V}_E$ at 8 μM, however no significant difference existed between the ages until 12 μM. Hamster preparations decreased $n\dot{V}_E$ significantly from baseline at low concentrations.

To depict the changes in T_I and T_E, pyramid plots are shown in Figure 3-3. In a pyramid plot, the upward slope from amplitude = 0 to the peak represents inspiratory duration (T_I). The downward slope from peak amplitude to amplitude = 0 represents expiratory duration (T_E). To calculate the values for T_I and T_E, normalized T_I and T_E means corrected for vehicle controls (in Appendix Table 6-1) were multiplied by the group mean absolute baseline value. In both ages of

rats, T_I did not deviate significantly from baseline values (Figure 3-3A, B). Conversely in young rats, T_E steadily increased with increasing concentrations of riluzole (downward slope shifts right along x-axis). In weaned rats, T_E also increased but changed very little. In response to increasing concentrations of riluzole, rat preparations preferentially decreased frequency by elongating the interburst interval. Hamsters (Figure 3-3C) increased both T_I and T_E (peak and downward slope shift right along x-axis) which resulted in the observed change in frequency.

3.2. Flufenamic acid application

Similar to riluzole, FFA had not been applied to the *in situ* preparation; previously reported concentrations applied to brainstem transverse slice preparations ranged 100 - 500 μM FFA (Pena *et al.*, 2004; Del Negro *et al.*, 2005). We applied FFA starting at 0.25 μM and increased the concentration of FFA until a significant response was obtained in the raw data.

Most preparations of weaned rats and hamsters continued producing fictive respiratory motor output until the highest concentration of FFA (25 μM) (Table 3-3). Furthermore, sixty percent of the young rat preparations also continued to generate phrenic motor output at 25 μM FFA. Representative raw and rectified, integrated neurograms are presented in Figure 3-4. Unlike the riluzole trials, all groups continue bursting at the highest concentration and all groups showed frequency increasing with increasing concentrations of FFA. This increase in frequency also was observed during vehicle control runs. Similarly, amplitude in all three groups decreased over time, which was also observed during vehicle controls.

Figure 3-5 shows the changes in normalized frequency (A), amplitude (B), and $n\dot{V}_E$ (C), corrected for vehicle controls, in response to increasing concentrations of FFA. Burst frequency (Figure 3-5A) was not significantly affected by the addition of FFA in any of the groups.

Amplitude (Figure 3-5B) decreased with increasing FFA concentration in all groups. Weaned rats decreased amplitude significantly from baseline at very low concentrations; however, amplitude was maintained at about 60% of baseline until 25 μM. Amplitude slowly decreased in young rat preparation and was significantly different from baseline after 10 μM. A significant difference exists between young and weaned rats at low concentrations of FFA. Hamster preparations maintained phrenic burst amplitude near baseline values.

Neural ventilation decreased significantly in weaned and young rats, particularly at higher concentrations, but $n\dot{V}_E$ was maintained around baseline in hamsters (Figure 3-5C).

Pyramid plots in Figure 3-6 depict the changes in T_I and T_E in response to increasing concentrations of FFA and were calculated as described in section 3.1 with the data in Appendix Table 6-2. In young rat preparations (Figure 3-6A), T_I decreased to 60% of baseline and T_E decreased to 35% of baseline. In contrast, T_I in weaned rat preparations (Figure 3-6B) did not change significantly from baseline; however, T_E tended to increase as FFA concentration increased. In hamsters (Figure 3-6C), T_I and T_E remained the same with increasing concentrations of FFA.

Greater concentrations of FFA have been applied in brainstem transverse slice preparations to completely eliminate I_{CAN} (Del Negro *et al.*, 2005; Pace *et al.*, 2007a); therefore, a small number of experiments were run in which concentrations of 25 – 100 μM FFA were applied only to weaned rat preparations in order to see if increasing FFA would result in a change in respiratory motor output. When FFA was applied to weaned rat preparations up to a concentration of 100 μM (Figure 3-7), only one third of preparations continued generating motor output while two thirds of the preparations ceased discharge at 50 μM. Frequency and amplitude significantly declined with increasing concentration; therefore, their product, $n\dot{V}_E$, also significantly declined.

3.3. Riluzole and FFA coapplication

We applied riluzole and FFA in combination to test the response of rats and hamsters to the elimination of both I_{NaP} and I_{CAN}. We expected that young rats and hamsters would have a greater decrease in fictive breathing resulting from a hypothesized greater dependence on I_{NaP} and I_{CAN} for respiratory rhythm generation. Six concentrations of the riluzole and FFA combination were applied, which had been calculated from the experiments where the drugs were applied individually to result in a 5, 10, 15, 20, 25 or 50% decrease in frequency and amplitude from baseline values.

3.3.1. Coapplication at 5% CO_2

Adding riluzole and FFA in combination to rat and hamster *in situ* preparations was effective in abolishing respiratory rhythm in some preparations and Table 3-4 gives the number of preparations that continued to produce phrenic bursting at the indicated concentrations of riluzole and FFA. No young rat preparations continued generating motor output at 20 μM riluzole + 15 μM FFA. Only 30% of weaned rats and 50% of hamster preparations continued generating bursts after the final concentration. In the example neurograms shown in Figure 3-8, neither the young rat or hamster preparation continued breathing after the coapplication of 20 μM riluzole + 15 μM FFA. The weaned rat preparation continued to breathe and frequency tended to remain at baseline values; however, amplitude was profoundly decreased. Before respiratory rhythm was abolished in young rat and hamster preparations, frequency of phrenic bursts was profoundly decreased and amplitude of phrenic bursts decreased.

Normalized frequency, amplitude, and $n\dot{V}_E$, corrected for vehicle controls, of the phrenic motor output are presented in Figure 3-9. Similar to riluzole trials, burst frequency (Figure 3-9A) of hamsters decreased significantly at lower concentrations of riluzole and FFA; 50% of baseline values was obtained at 7.5 μM riluzole + 5 μM FFA. The frequency of phrenic bursts also decreased significantly in young rat preparations. Weaned rat preparations reduced frequency to below 50% at 20 μM riluzole +15 μM FFA. Significant differences exist between young and weaned rats at higher concentrations as weaned rats maintained frequency at concentrations where young rat burst frequency declined.

The amplitude (Figure 3-9B) of phrenic bursting decreased significantly in all groups. Young and weaned rat preparations decreased amplitude at low concentrations, particularly in young rats (to 14% of baseline). In rats, the phrenic burst amplitude typically reached zero while frequency decreased less. Hamster preparations decreased amplitude the least.

Neural ventilation (Figure 3-9C) significantly decreased in all groups in response to increasing concentrations of riluzole and FFA. The greatest decrease in $n\dot{V}_E$ occurred in weaned rat preparations where $n\dot{V}_E$ reached <10% of baseline. However, the drop in $n\dot{V}_E$ was due to different components (though the effects are offset so $n\dot{V}_E$ was similarly affected in all groups). In

hamster preparations, decreased frequency contributed more to the decrease in $n\dot{V}_E$; in rat preparations, decreased amplitude contributed to the decrease in $n\dot{V}_E$.

The response of $n\dot{V}_E$ in response to individual application of riluzole and FFA were added to calculate expected $n\dot{V}_E$ values based on the assumption that riluzole and FFA effects are additive. Figure 3-10 compares the expected values with the actual response of $n\dot{V}_E$. In all groups, the actual response to the coapplication of riluzole and FFA was more profound than expected. The only exception was in hamster preparations at 6 μM RIL + 2.5 μM FFA where $n\dot{V}_E$ was expected to be lower than the actual result.

Pyramid plots (Figure 3-11) for young and weaned rats and weaned hamster preparations were calculated using data from Appendix Table 6-3 as described in section 3.1. In young and weaned rat preparations (Figure 3-11A,B), T_I stayed at baseline values. In both young and weaned rat groups, T_E increased as concentrations of riluzole and FFA increased. In hamster preparations (Figure 3-11C), T_I remained around baseline values and T_E increased dramatically up to 37x baseline values at 10 μM riluzole + 8 μM FFA, after which T_E values decreased. In response to increases concentrations of riluzole and FFA in combination, rats and hamsters decreased frequency by increasing the interburst interval (T_E).

3.3.2. Coapplication at 7% CO_2

Del Negro and colleagues (2005) showed that increasing drive to the respiratory network (by application of substance P) after the abolition of respiratory rhythm by coapplication of riluzole and FFA rescued respiratory rhythm. In order to increase respiratory drive in the *in situ* preparation, we increased the proportion of CO_2 bubbling in the perfusate to 7% (93% O_2) and expected that respiratory rhythm would be greater during coapplication of riluzole and FFA than the preparations exposed to 5% CO_2. Preparations were exposed to perfusate equilibrated with 7% CO_2 (93% O_2) in order to increase the respiratory drive when the combination of riluzole and FFA were administered. For these preparations, 15% of young rat, 63% of hamster and all weaned rat preparations continued generating motor output after the final concentration of the drug combination (Δ Amplitude is the relative change in phrenic burst amplitude. Dashed line represents baseline TI. Please note different times axis for hamsters.

Table 3-5). At 5% CO_2, no young rat preparations continued bursting after the final concentration of the cocktail (Table 3-4).

The baseline values for preparations perfused with 7% CO_2 were calculated by dividing the 7% CO_2 (high drive) value by the 5% CO_2 (normal drive) value prior to drug application. Table 3-6 shows the frequency, T_I and T_E baseline (absolute) values for preparations at 5% or 7% CO_2. Frequency in rat preparations tended to increase when exposed to 7% CO_2 (significantly in young rats preparations) while frequency in hamsters appeared to stay the same. These changes in frequency appear to be due to both shortening of the inspiratory and expiratory duration.

Frequency (Figure 3-12) of phrenic bursts in all high drive preparations remained higher than the frequency in normal drive preparations. Within all groups, phrenic burst frequency decreased at a similar rate for both 5% and 7% CO_2 following coapplication of riluzole and FFA. In young rats (Figure 3-12A), frequency was significantly higher at low concentrations for 7% CO_2 than 5% CO_2. This difference disappeared at higher concentrations. No significant difference exists between high drive and normal drive preparations in weaned rats (Figure 3-12B) and hamsters (Figure 3-12C). Increasing respiratory drive by stimulating chemoreceptors did not negate the effect of riluzole or FFA in weaned rats or hamsters on frequency.

The amplitude of phrenic nerve bursts (Figure 3-13) in young rat preparations (Figure 3-13A) decreased at high and normal drive at a similar rate. In weaned rats (Figure 3-13B), the amplitude of high drive preparations was significantly greater than the amplitude values for normal drive preparations. The weaned rat preparations at 7% CO_2 maintained amplitude around baseline values, while the normal drive amplitude fell from baseline. In hamsters (Figure 3-13C), phrenic burst amplitude of high and normal drive preparations was the same and remained around baseline values. No significant difference existed between 5% CO_2 and 7% CO_2 preparations for young rats or hamsters.

In all groups, $n\dot{V}_E$ (Figure 3-14) decreased significantly from baseline values in high drive preparations as concentrations of the drug combination increased. In weaned rat preparations (Figure 3-14B), ventilation was increased significantly in 7% CO_2. In young rats and hamsters (Figure 3-14A, C), the ventilation of high drive preparations was very similar to the values for

normal drive preparations and decreased from baseline values at the same rate. Exposing *in situ* preparations to 7% CO_2 and coapplication of riluzole and FFA significantly increased ventilation in weaned rats over the majority of concentrations and seemed to have no significant effect on the response of young rats or hamsters to riluzole and FFA.

Table 3-1: Mean and the range of baseline phrenic nerve burst frequency for young rats, weaned rats and weaned hamsters. The values are ± standard error.

Age group	Mean (bursts/min)	Range (bursts/min)
Young rat	19.4 ± 1.0	6.4 - 51.5
Weaned rat	18.1 ± 0.9	6.6 - 35.3
Weaned hamster	46.6 ± 4.2	13.4 - 128.6

Table 3-2: The number of animals with phrenic nerve activity at indicated concentrations of riluzole.

	Number of animals		
[RIL] (μM)	Young rats	Weaned rats	Weaned hamsters
0.0	11	6	6
0.2	11	6	6
1.0	11	6	6
2.0	11	6	6
4.0	11	6	6
6.0	11	6	5
8.0	11	6	3
10.0	10	6	2
12.0	5	6	1
14.0	3	6	1
16.0	3	6	0
18.0	3	6	0
20.0	3	6	0

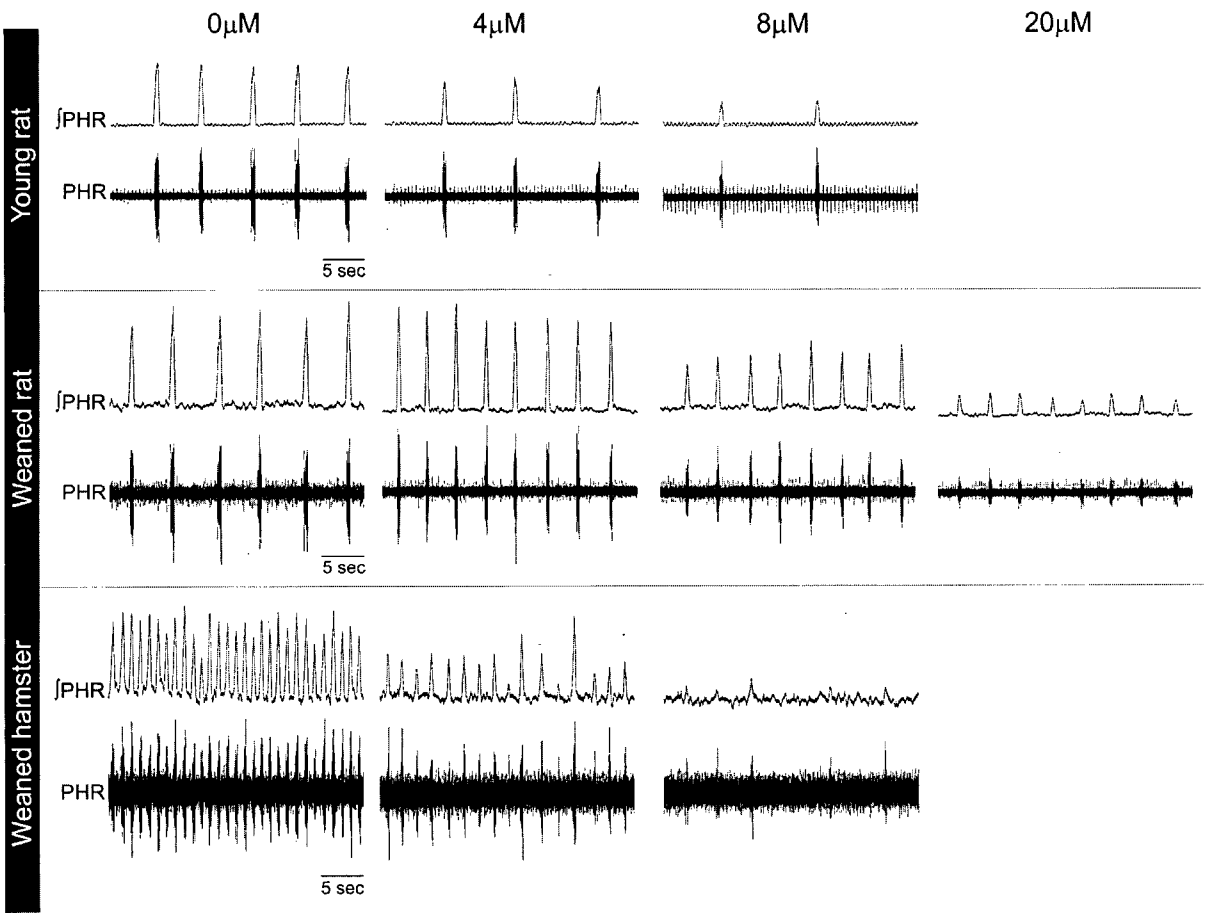

Figure 3-1: Thirty second representative raw (PHR) and rectified integrated (∫PHR) neurograms of PHR nerve activity in response to increasing concentrations of riluzole.
Top series is from a young rat (12 PND), middle series from a weaned rat (25 PND), bottom series from a weaned hamster (26 PND).

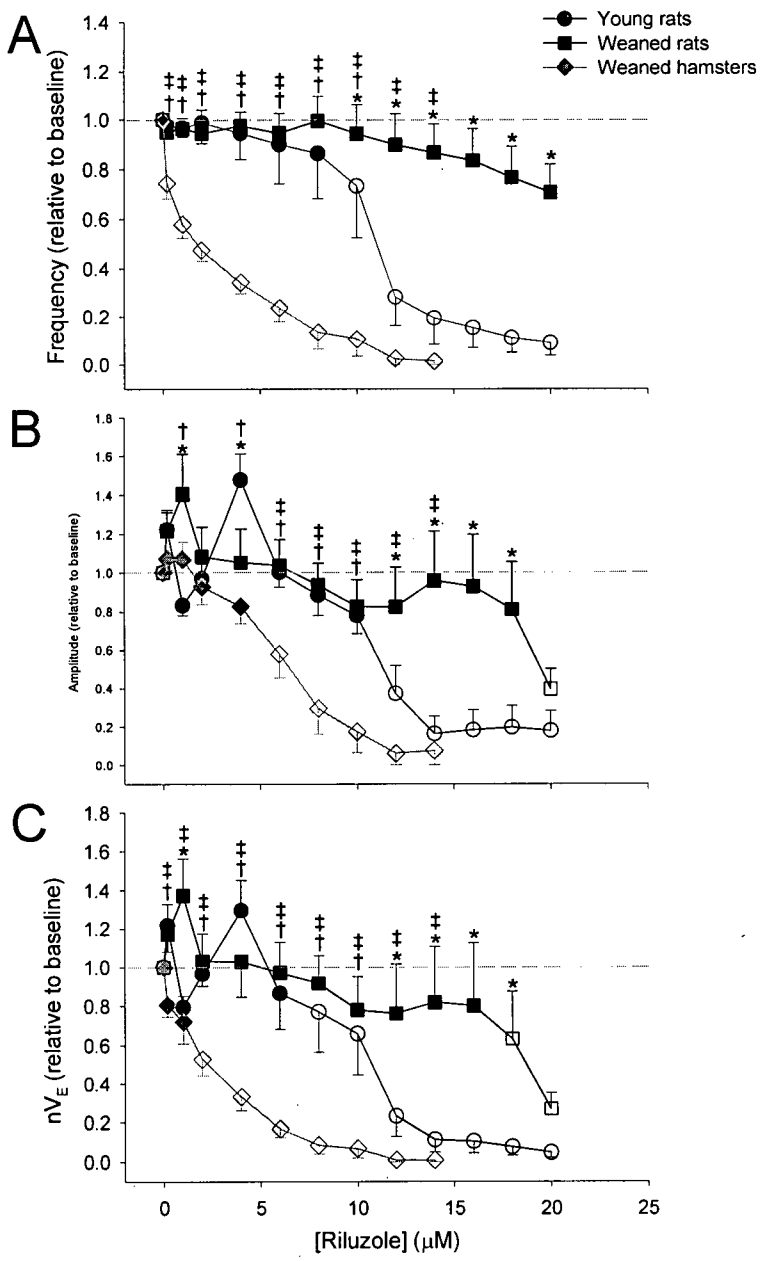

Figure 3-2: The change in phrenic nerve burst frequency (A), amplitude (B), and neural ventilation ($n\dot{V}_E$, C), corrected for vehicle controls, in response to increasing concentrations of riluzole.

Young rats (n=11) are represented by circles (•); weaned rats (n=6) are represented by squares (■); weaned hamsters (n=6) are represented by diamonds (♦). Open shapes indicate significant differences from 0 μM (denoted by grey dashed line). Asterisks (*) denote significant differences between young and weaned rats. Daggers (†) denote significant difference between young rats and weaned hamsters; double daggers (‡) denote significant differences between weaned rats and hamsters.

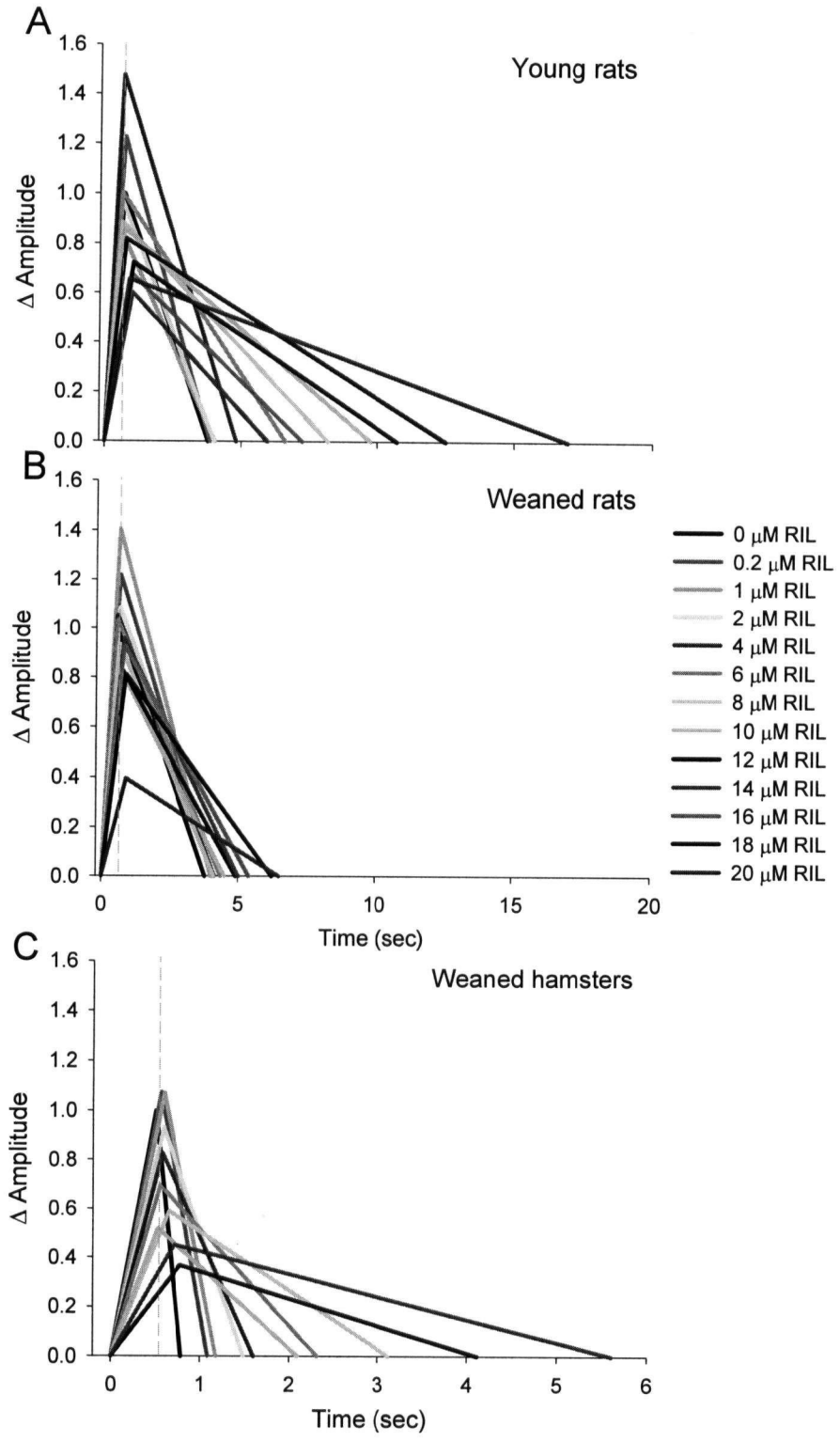

Figure 3-3: Pyramid plots for young rats (A), weaned rats (B) and weaned hamsters (C) for increasing concentrations of riluzole (RIL).

Δ Amplitude is the relative change in phrenic burst amplitude. Dashed line represents baseline T_I. Please note different times axis for hamsters.

Table 3-3: The number of animals with phrenic nerve activity at indicated concentrations of FFA.

Concentration (μM)	Number of animals		
	Young rats	Weaned rats	Weaned hamsters
0.0	10	7	7
0.25	10	7	7
1.25	10	7	7
2.5	10	7	7
5.0	10	7	7
7.5	10	7	7
10.0	9	7	7
12.5	8	7	7
15.0	8	7	7
17.5	6	7	7
20.0	6	7	7
22.5	6	7	6
25.0	6	7	6

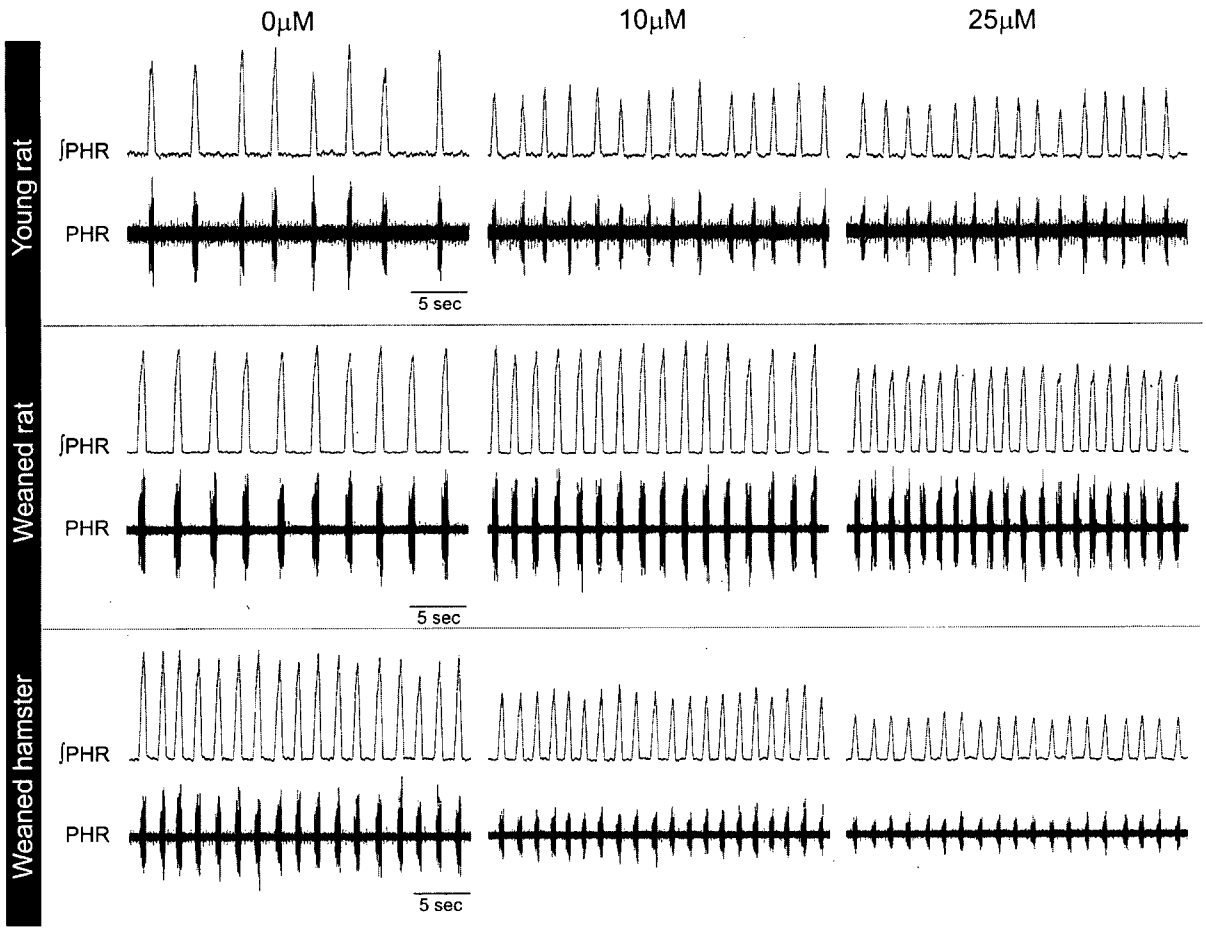

Figure 3-4: Thirty second representative raw (PHR) and rectified integrated (∫PHR) neurograms of PHR nerve activity in response to increasing concentrations of FFA.
Top series is from a young rat (14 PND), middle series from a weaned rat (25 PND), bottom series from a weaned hamster (29 PND).

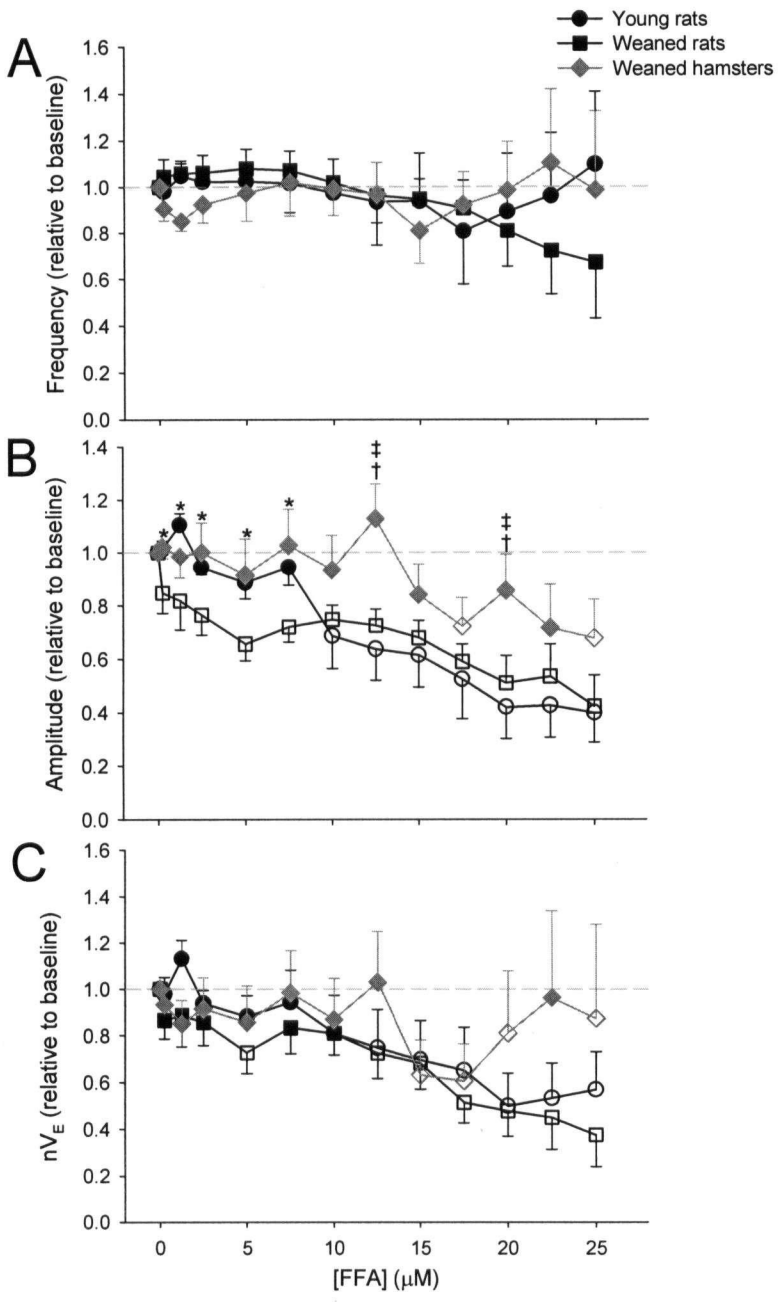

Figure 3-5: The change in phrenic nerve burst frequency (A), amplitude (B), and neural ventilation ($n\dot{V}_E$, C), corrected for vehicle controls, in response to increasing concentrations of FFA.

Young rats (n=10) are represented by circles (•); weaned rats (n=7) are represented by squares (■); weaned hamsters (n=7) are represented by diamonds (♦). Open shapes indicate significant differences from 0 **μ**M (denoted by grey dashed line). Asterisks (*) denote significant differences between young and weaned rats. Daggers (†) denote significant difference between young rats and weaned hamsters; double daggers (‡) denote significant differences between weaned rats and hamsters.

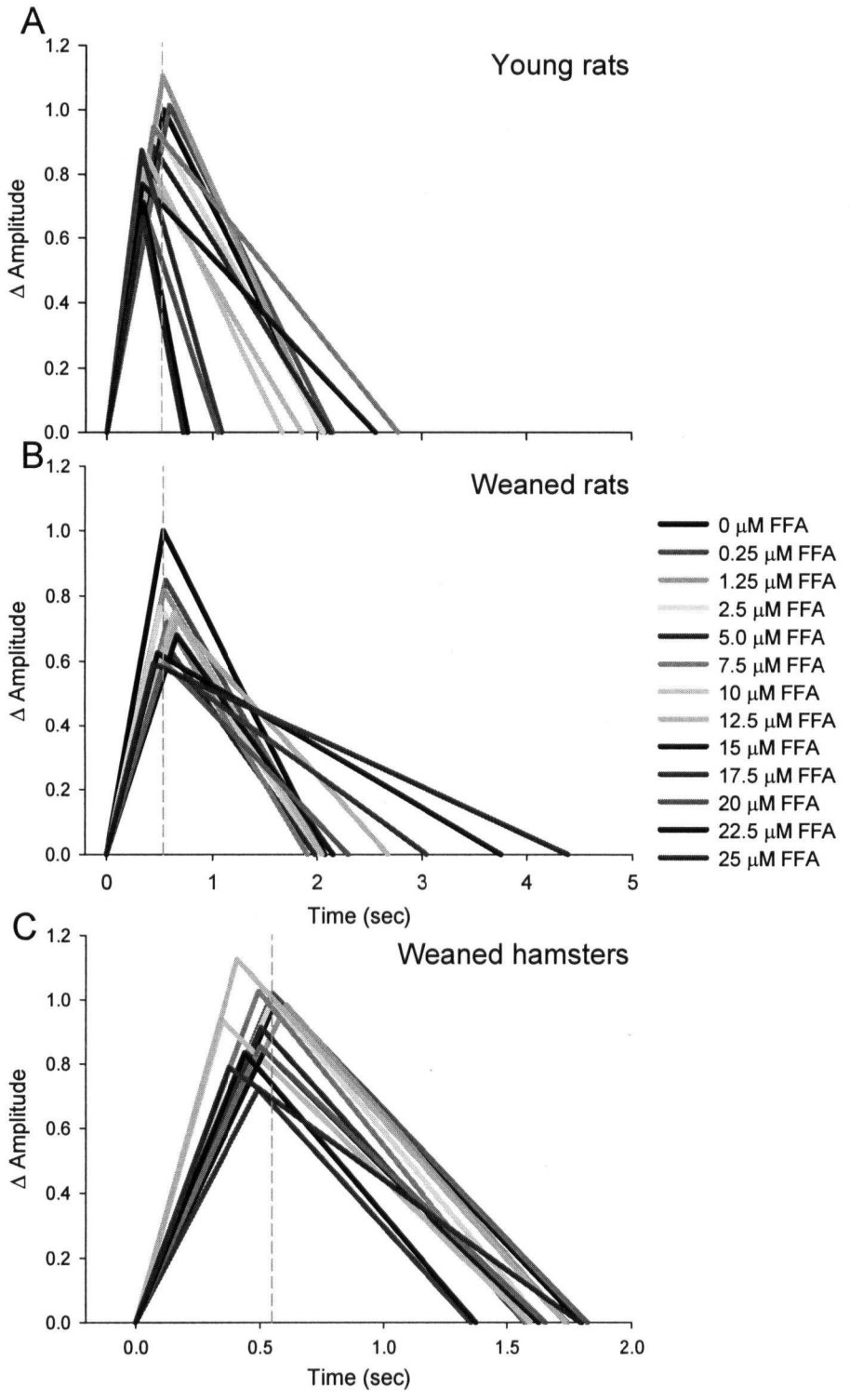

Figure 3-6: Pyramid plots for young rats (A), weaned rats (B) and weaned hamsters (C) for increasing concentrations of FFA.
Δ Amplitude is the relative change in phrenic burst amplitude. Dashed line represents baseline T_I. Please note different times axis for hamsters.

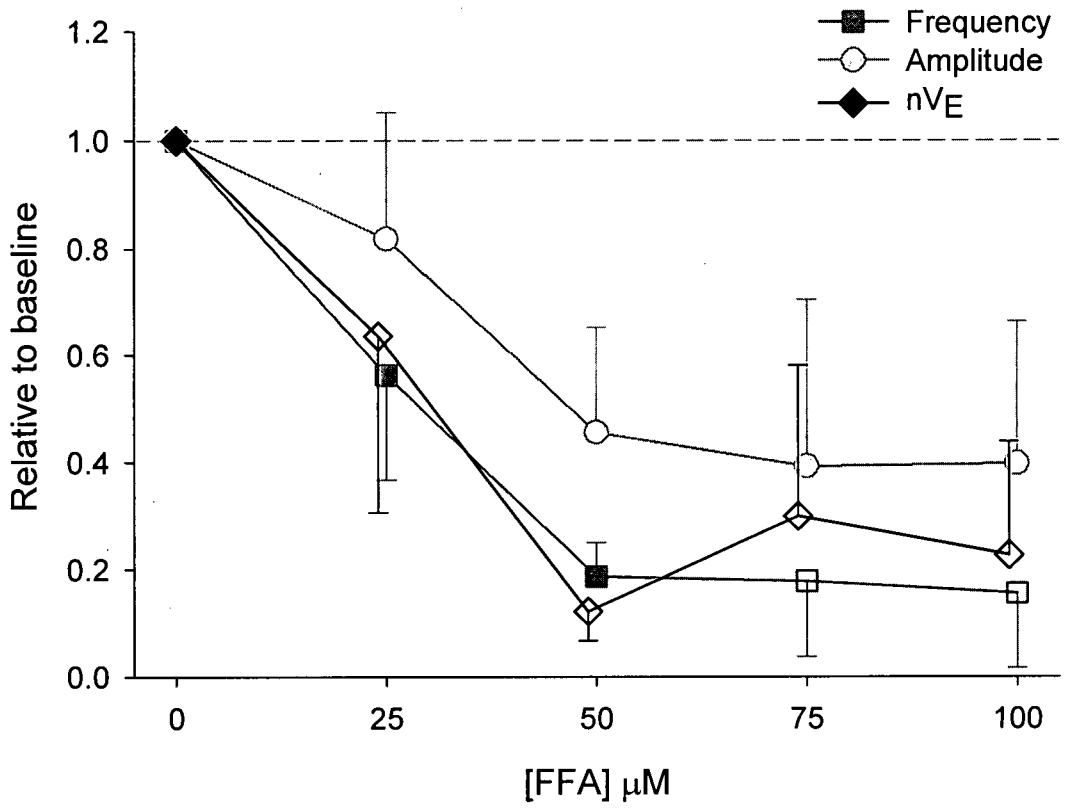

Figure 3-7: Frequency, amplitude and neural ventilation ($n\dot{V}_E$) all declined as FFA concentration increased in weaned rat preparations (n=6).
Open shapes indicate significant difference from 0 μM.

Table 3-4: Number of preparations producing respiratory rhythm during coapplication of riluzole and FFA.

Concentration [RIL]+[FFA]	Number of animals: Young rats	Weaned rats	Weaned hamsters
0 μM+0 μM	16	10	8
6 μM+2.5 μM	16	9	8
7.5 μM+5 μM	14	9	7
9 μM+6 μM	13	9	7
10 μM+8 μM	7	9	6
12 μM+10 μM	4	10*	6
20 μM+15 μM	0	3	4

* the values from one preparation in the weaned rat group only had 0 μM RIL + FFA, 12 μM+10 μM and 20 μM+15 μM applied.

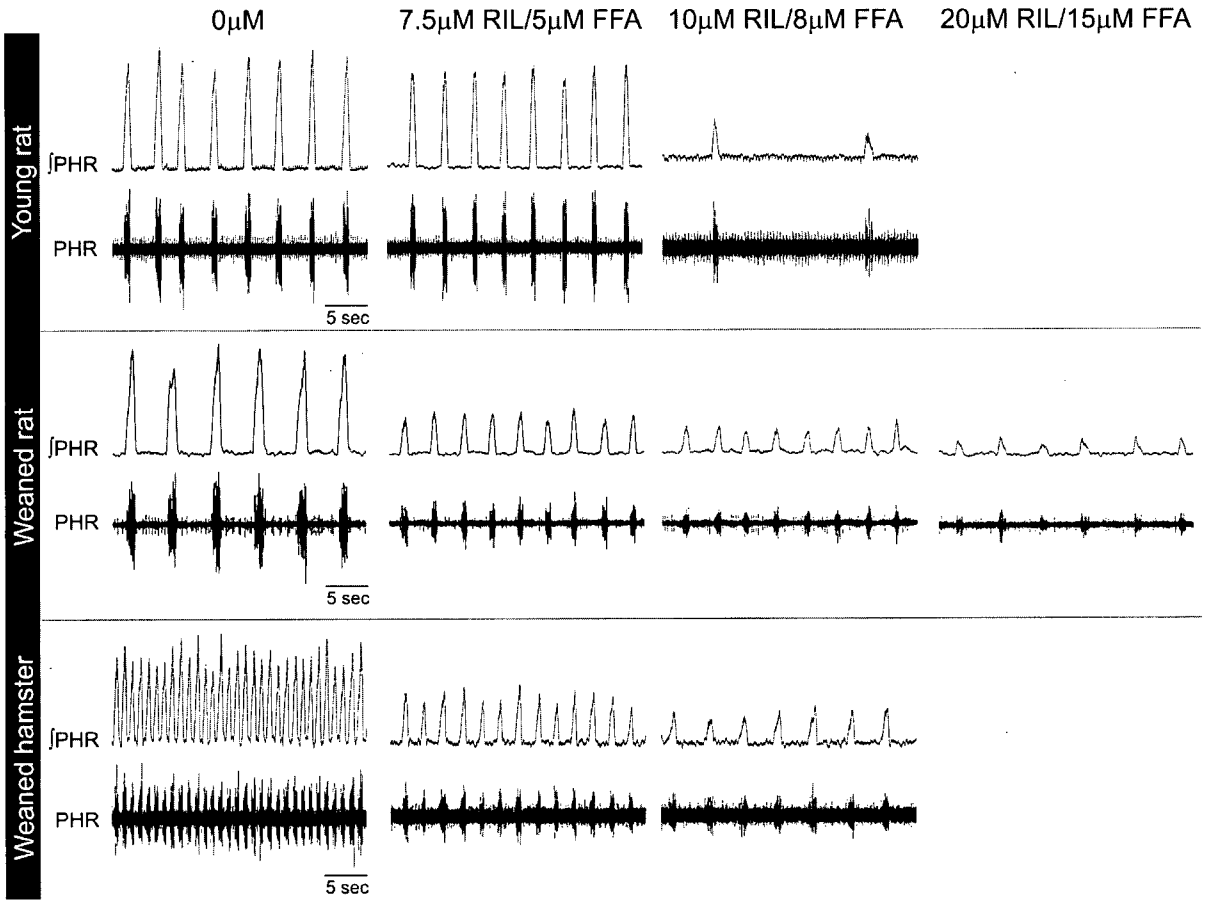

Figure 3-8: Thirty second representative raw (PHR) and rectified integrated (∫PHR) neurograms of PHR nerve activity in response to increasing concentrations of riluzole and FFA.
Top series is from a young rat (12 PND), middle series from a weaned rat (27 PND), bottom series from a weaned hamster (25 PND).

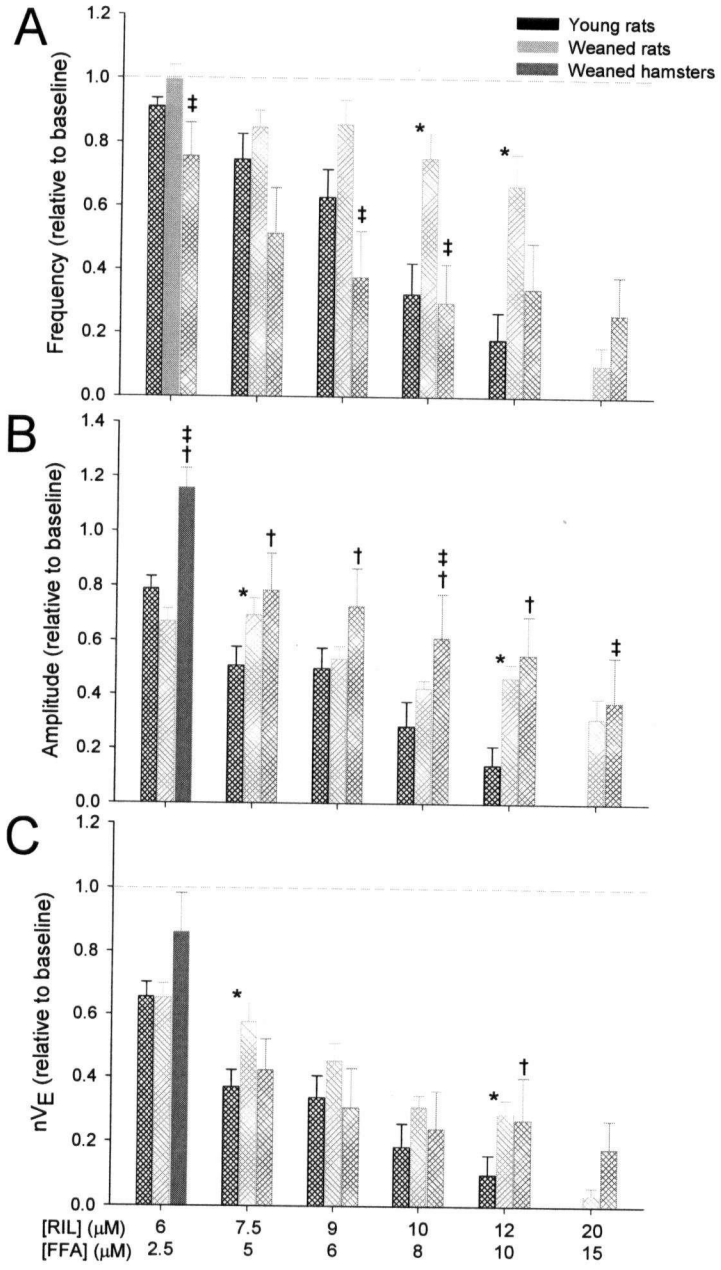

Figure 3-9: The change in phrenic nerve burst frequency (A) and amplitude (B), and neural ventilation ($n\dot{V}_E$, C) corrected for vehicle controls, in response to increasing concentrations of riluzole and FFA.

Young rats (n=16) are represented by black bars (■); weaned rats (n=10) are represented by light grey bars (■); weaned hamsters (n=8) are represented by dark grey bars (■). Hashed bars indicate significant differences from 0 μM (denoted by grey dashed line). Asterisks (*) denote significant differences between young and weaned rats. Daggers (†) denote significant difference between young rats and weaned hamsters; double daggers (‡) denote significant differences between weaned rats and hamsters.

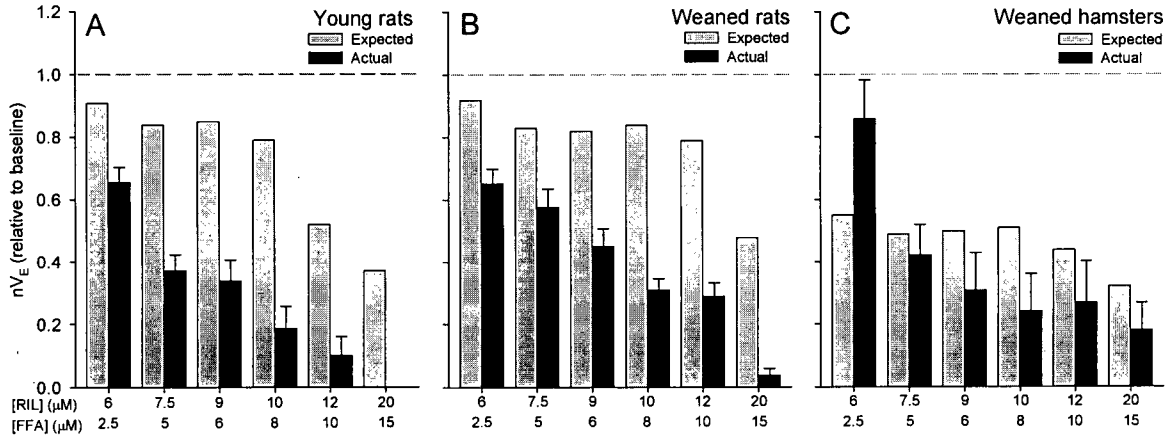

Figure 3-10: Expected values for neural ventilation ($n\dot{V}_E$) based on additive action of riluzole and FFA compared to the actual $n\dot{V}_E$ for young rats (A), weaned rats (B) and weaned hamsters (C). Dashed line = baseline = 1.0.

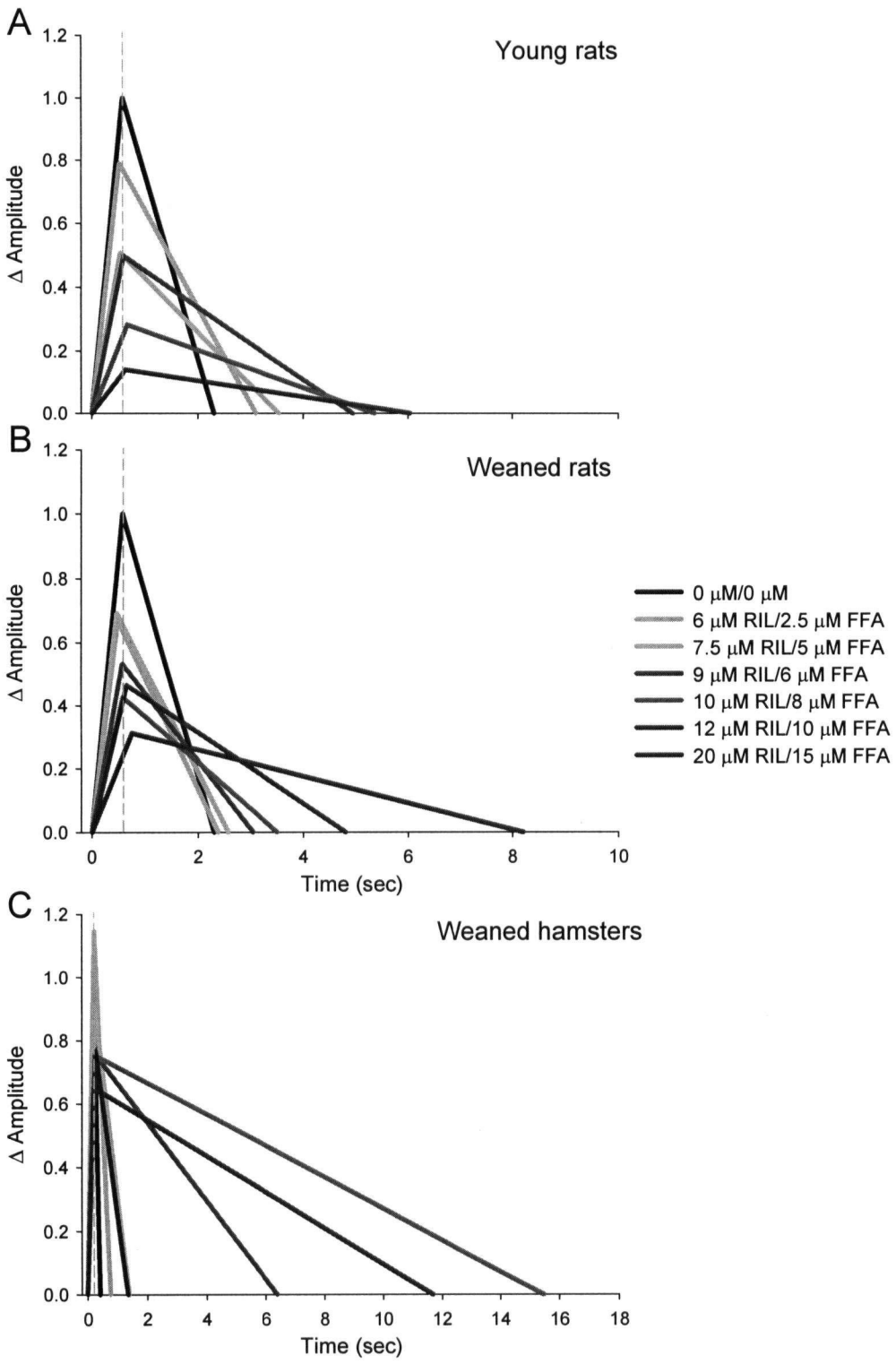

Figure 3-11: Pyramid plots for young rats (A), weaned rats (B) and weaned hamsters (C) for increasing concentrations of riluzole and FFA combination.
Δ Amplitude is the relative change in phrenic burst amplitude. Dashed line represents baseline T_I. Please note different times axis for hamsters.

Table 3-5: Number of preparations exposed to 7% CO_2 producing respiratory rhythm during coapplication of riluzole and FFA.

Concentration [RIL]+[FFA]	Number of animals		
	Young rats	Weaned rats	Weaned hamsters
0 μM+0 μM	13	6	8
6 μM+2.5 μM	13	6	8
7.5 μM+5 μM	12	6	8
9 μM+6 μM	10	6	8
10 μM+8 μM	7	6	8
12 μM+10 μM	7	6	8
20 μM+15 μM	2	6	5

Table 3-6: Alterations in phrenic nerve burst frequency, T_I and T_E of young rat, weaned rat and weaned hamster preparations exposed to 5% CO_2 or 7% CO_2. Values are expressed as means±standard error. *N*=number of preparations.

	Frequency (bursts/min)		T_I (sec)		T_E (sec)	
	5%	7%	5%	7%	5%	7%
Young rat *N*=13	17.5 ± 1.78	22.6 ± 2.22	0.48 ± 0.02	0.41 ± 0.04	3.67 ± 0.67	2.80 ± 0.53
Weaned rat *N*=6	17.1 ± 6.4	21.4 ± 3.4	0.82 ± 0.33	0.64 ± 0.21	3.41 ± 2.58	2.23 ± 0.65
Hamster *N*=8	29.4 ± 4.6	29.2 ± 3.1	0.57 ± 0.07	0.60 ± 0.08	1.79 ± 0.27	1.66 ± 0.28

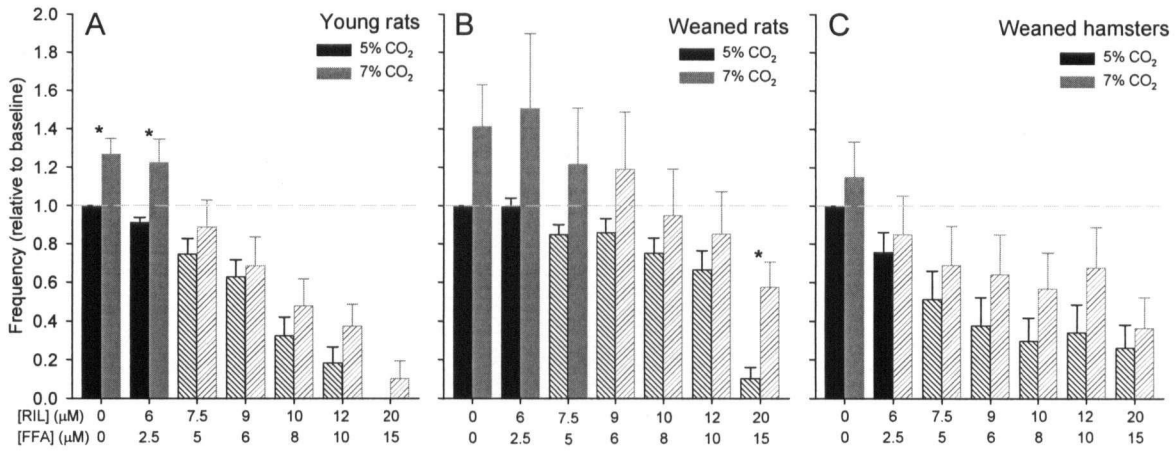

Figure 3-12: Changes in frequency, corrected for vehicle controls, for young rat (A), weaned rat (B) and hamster (C) preparations exposed to perfusate equilibrated with 5% CO_2 or 7% CO_2 and coapplication of riluzole and FFA.
Preparations at 5% are represented in black. Preparations at 7% for young rats (n=13), weaned rats (n=6) and hamsters (n=8) are represented in grey. Hashed bars indicate significant difference from value at 0 μM (denoted by grey dashed line). Asterisks (*) denote significant differences between 5% and 7% CO_2 preparations.

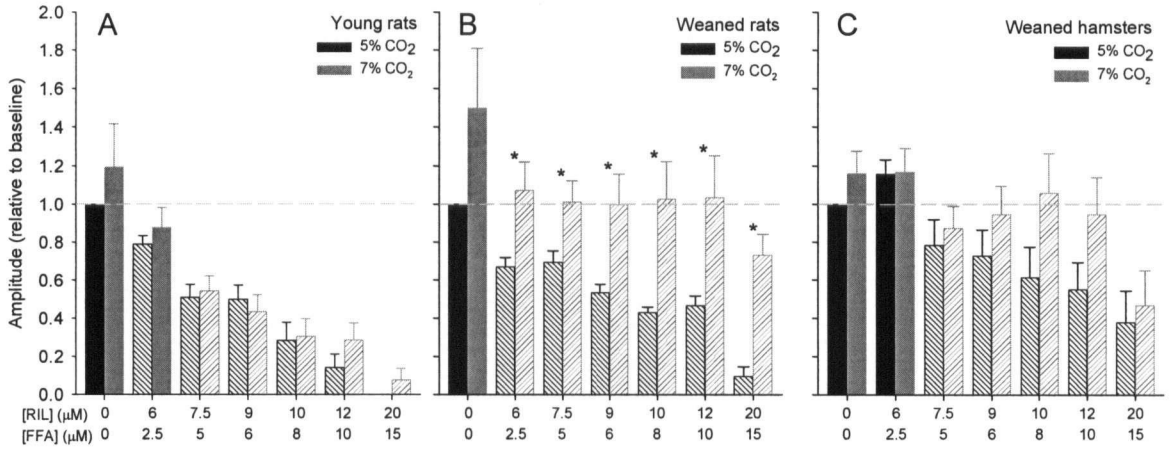

Figure 3-13: Changes in amplitude, corrected for vehicle controls, for young rat (A), weaned rat (B) and hamster (C) preparations exposed to perfusate equilibrated with 5% CO_2 or 7% CO_2 and coapplication of riluzole and FFA.
Preparations at 5% are represented in black. Preparations at 7% for young rats (n=13), weaned rats (n=6) and hamsters (n=8) are represented in grey. Hashed bars indicate significant difference from value at 0 μM (denoted by grey dashed line). Asterisks (*) denote significant differences between 5% and 7% CO_2 preparations.

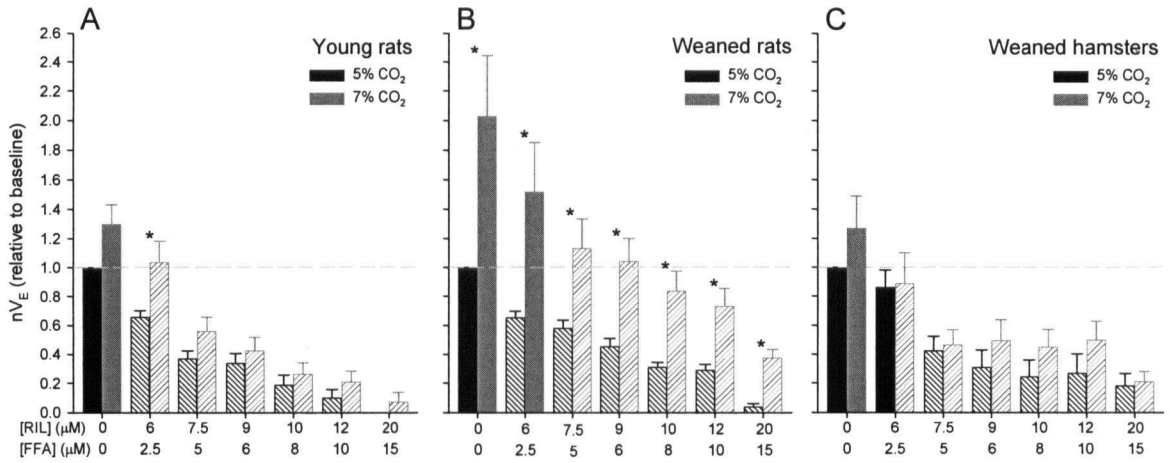

Figure 3-14: Changes in neural ventilation ($n\dot{V}_E$), corrected for vehicle controls, for young rat (A), weaned rat (B) and hamster (C) preparations exposed to perfusate equilibrated with 5% CO_2 or 7% CO_2 and coapplication of riluzole and FFA.
Preparations at 5% are represented in black. Preparations at 7% for young rats (n=13), weaned rats (n=6) and hamsters (n=8) are represented in grey. Hashed bars indicate significant difference from value at 0 μM (denoted by grey dashed line). Asterisks (*) denote significant differences between 5% and 7% CO_2 preparations.

4. Discussion

We hypothesize that phylogenetic and ontogenetic differences occur in the roles of I_{NaP} and I_{CAN} such that hamsters and young rats have a greater reliance on I_{NaP} and I_{CAN} for respiratory rhythm generation than weaned rats. Riluzole (an I_{NaP} blocker) and FFA (an I_{CAN} blocker) were applied to the *in situ* preparation in young (12 - 14 PND) and weaned (23 - 30 PND) rats and weaned hamsters (>23 PND).

Our results indicate that hamsters depend on I_{NaP} and I_{CAN} to a greater extent for respiratory rhythm generation than rats. The fictive breathing frequency of hamster preparations significantly decreased during application of riluzole and coapplicaton of riluzole and FFA to the *in situ* preparation. This change in frequency was significantly different from the response of young and weaned rats. Fictive respiration amplitude in hamsters was less affected by the coapplication of riluzole and FFA than in rats. Total neural ventilation was significantly lower in hamsters than rats during application of riluzole, but no significant difference exists during the coapplication of riluzole and FFA.

The frequency, amplitude and neural ventilation of young rats also tended to be affected more by the application of riluzole and FFA than those of weaned rats. For instance, young rats, like hamsters, depend to a greater extent on I_{NaP} and I_{CAN} for respiratory rhythm generation than weaned rats. These data indicate that a change in the role of I_{NaP} and I_{CAN} in the CRG occurs during development.

Increasing excitatory drive to the CRG by increasing CO_2 significantly increased ventilation in weaned rats only. These data suggest that in weaned rats other sources of respiratory drive may compliment the roles of I_{NaP} and I_{CAN}.

4.1. Technical considerations

Riluzole binds to Na^+ and K^+ channels in their inactivated state (but not their resting or open state) (Benoit & Escande, 1993)(Benoit & Escande, 1991)(Doble, 1996). Although riluzole inhibits both Na^+ and K^+ currents, it preferentially binds to Na^+ channels and is estimated to have 300 times more affinity for inactivated state Na^+ channels than resting channels (Benoit & Escande, 1991)(Benoit & Escande, 1993). By preferentially binding the inactivated state of Na^+

channels, riluzole shifts the membrane potential to a more hyperpolarized voltage, resulting in the inactivation of I_{NaP}. [As described in section 1.3, I_{NaP} is active at more depolarized potentials.] (Ptak *et al.*, 2005; Feldman & Del Negro, 2006). Riluzole also interferes with glutamate signalling, which further affects the activation of Ca^{2+} and Na^{+} currents (Doble, 1996). However, ample evidence shows that at low concentrations for short periods of time, riluzole is specific for I_{NaP} (EC50 = 3 μM for *in vitro* brainstem transverse slices, = 2 μM for cortical slices) (Urbani & Belluzzi, 2000)(Del Negro *et al.*, 2005). At the concentrations used in this study (0.5 μM - 20 μM), while riluzole may have been acting on several channels and currents, it will have certainly blocked I_{NaP}.

The channels that produce the I_{CAN} current are most likely members of the TRPM family (transient receptor potential-melastatin) which are inhibited by FFA (100 μM) (Launay *et al.*, 2002; Guinamard *et al.*, 2004). In *in vitro* transverse slices, bath applying 100 μM FFA was not sufficient to completely eliminate I_{CAN} (Pace *et al.*, 2007a). Concentrations of FFA that do completely abolish I_{CAN} also will block gap junctions reversibly (EC_{50} = 40 μM - 47 μM) (Srinivas & Spray, 2003)(Harks *et al.*, 2001), reversibly inhibit Ca^{2+}-dependent and voltage-dependent Cl^{-} channels (White & Aylwin, 1990), and stimulate or inhibit (depending on concentration) large conductance Ca^{2+}-activated K^{+} channels which may influence neuronal firing (Ottolia & Toro, 1994)(Li *et al.*, 1998)(Farrugia *et al.*, 1993)(Kochetkov *et al.*, 2000). However, many investigators use FFA with the understanding that results regarding the elimination of I_{CAN} must be cautiously interpreted due to the multiple and incomplete actions of FFA.

Previous studies have reported that riluzole only affected the respiratory frequency of hypoxia-induced gasping (Paton *et al.*, 2006). The frequency response to riluzole seen in our hamster and young rat preparations might suggest therefore that our preparations are hypoxic and the rhythm we recorded was gasping, and not normoxic breathing. For this reason, we recorded from the CVN to validate the stability and viability of the hamster and young rat *in situ* preparations (see Methods for explanation). The recordings of CVN activity (Figure 2-3B, C) showed that our young rat and hamster preparations were stable and viable because the preparations exhibited the three neural phases of respiration (inspiratory, post-inspiratory and expiratory). Therefore, we can confirm that the rhythms we recorded were not gasping and

attribute any decreases in frequency to the action of riluzole on I_{NaP} (and other currents) rather than poor stability of the preparations.

In our measurements of respiratory variables, frequency of phrenic discharge indicates the rhythm outputted by the CRG. Therefore, to change frequency, thus rhythm, requires bringing membrane potential to threshold either more quickly or more slowly. Amplitude, in this study, does not refer to rhythm but to the net motor output generated by the entire respiratory network. To change amplitude implies that either fewer respiratory neurons are active or fewer repetitive bursts occur per breath per bursting neuron. Therefore, if elimination of I_{NaP} and I_{CAN} results in a change in frequency, rhythmogenesis at the CRG would be affected; whereas, a decrease in amplitude would indicate that the elimination of I_{NaP} and I_{CAN} has decreased the excitability of respiratory network.

4.2. Phylogenetic differences in I_{NaP} and I_{CAN} contribution to rhythm generation

Hamsters are permissive hibernators that require specific cues, such as water deprivation and shorter photoperiods, to induce hibernation (Ueda & Ibuka, 1995) while rats do not show this type of dormancy. Hamsters are also fossorial species exhibiting adaptations to living in hypoxic, hypercapnic burrow environments (Walker *et al.*, 1985) in addition to adaptations for hibernation.

4.2.1. Hamsters require I_{NaP} to set respiratory rhythm

Using the *in situ* preparation, eliminating I_{NaP} by applying riluzole in age-matched rats and hamsters had different concentration-dependent effects. No hamster preparations continued generating fictive breathing past 14 μM riluzole while weaned rats continued fictive breathing until 20 μM riluzole. Application of riluzole resulted in a profound decrease in phrenic burst frequency of hamster preparations at very low concentrations (Figure 3-2A). The concentrations that yielded a 50% decrease in phrenic burst frequency (1 – 2 μM) would have specifically blocked only I_{NaP} (Urbani & Belluzzi, 2000; Del Negro *et al.*, 2005). Frequency in weaned rats did not change significantly from baseline values at these concentrations. That riluzole affects frequency in hamsters, not rats, was observed in the isolated brainstem-spinal cord preparation in early post-natal development (0 – 4 PND) (Marshall, 2005), suggesting that the difference exists at birth.

This response of the hamsters is different than all existing reports of riluzole application in mice and rats. Because riluzole had no effect on burst frequency in rat and mouse brainstem transverse slices, *in situ* preparations or intact rats, I_{NaP} is not considered necessary for respiratory rhythm generation (Del Negro *et al.*, 2005)(Paton *et al.*, 2006). When rhythm has been abolished, the effect had been attributed to the non-specific actions of riluzole at the high concentrations used (10 - 20 μM) (Del Negro *et al.*, 2005). The response of the *in situ* rat preparations in this study is consistent with the present literature because frequency did not change significantly with increasing riluzole. However, our data differ for hamsters suggesting that the CRG is being affected by the application of riluzole and that in hamsters I_{NaP} plays an important role in neurons that set respiratory rhythm.

In contrast with the drastic effect of eliminating I_{NaP}, FFA application had no significant effect on frequency in either hamsters or rats (Figure 3-5A) until concentrations >25 μM. Between 25 - 100 μM, FFA application resulted in the abolition of fictive breathing in most of the preparations through a decrease in frequency. At concentrations >25 μM, FFA will block not only I_{CAN} but also will interfere with various Ca^{2+}, Cl^- and K^+ currents and gap junctions (described in section 4.1) (White & Aylwin, 1990; Farrugia *et al.*, 1993; Ottolia & Toro, 1994; Li *et al.*, 1998; Harks *et al.*, 2001; Stumpff *et al.*, 2001; Srinivas & Spray, 2003). Application of FFA less than 25 μM most likely led to decreased excitability of the neuronal network which resulted in the decline in net motor output but had less effect on frequency in both rats and hamsters. The minor effect of FFA on frequency in our study is in accord with current literature that also does not report FFA having a frequency effect (Pena *et al.*, 2004; Pace *et al.*, 2007a).

When riluzole and FFA were coapplied, phrenic burst frequency in hamsters decreased significantly at low doses while the frequency in rat preparations was unchanged (Figure 3-9A). However, when compared to the decrease in frequency in response to riluzole alone, frequency in hamster preparations did not decline as much during coapplication at the corresponding concentrations. For instance, 50% of hamster preparations were able to continue fictive breathing during the coapplication of riluzole and FFA. The last concentration of riluzole in the combination is 20 μM. When riluzole was applied individually, no hamster preparations continued fictive breathing past 14 μM riluzole. This result suggests that FFA may mitigate some

of the effects of eliminating I_{NaP} in hamsters. FFA is known to block gap junctions (Harks *et al.*, 2001; Srinivas & Spray, 2003) and blockade of gap junctions in the *in situ* preparation has been shown to lead to increased phrenic burst frequency (Solomon *et al.*, 2003), which may be one mechanism by which FFA could negate some of the effects of eliminating I_{NaP} on frequency. Also, at the majority of the concentrations applied (2.5 - 15 μM), FFA would stimulate large conductance Ca^{2+}-activated K^+ channels (between 5 - 10 μM) (Kochetkov *et al.*, 2000), which may counteract the effect of riluzole in decreasing neuronal excitability, and result in less of a decline in frequency.

In contrast with the hamster, coapplication of riluzole and FFA in rat preparations led to a greater decrease in fictive breathing: only 30% of weaned rats continued generating phrenic bursts, whereas during riluzole alone, all weaned rats continued bursting at these concentrations (Table 3-4). In addition, in weaned rats, 12 μM riluzole only resulted in a 10% reduction in frequency; however when 12 μM riluzole was coapplied with 10 μM FFA, frequency was reduced by 34%. The ability of the coapplication of riluzole and FFA to reduce the frequency of the respiratory rhythm in our study corresponds with reports in brainstem transverse slice preparations and intact animals where respiratory motor output was abolished when riluzole and FFA were coapplied but not when applied individually (Pena *et al.*, 2004; Del Negro *et al.*, 2005; Pace *et al.*, 2007b; Pena & Aguileta, 2007). However, in these studies, the concentration of FFA used was very high (100 - 500 μM), and motor output declined due to falling amplitude, not frequency (Pena *et al.*, 2004; Del Negro *et al.*, 2005; Pace *et al.*, 2007b; Pena & Aguileta, 2007). Therefore, the eliminating I_{NaP} and I_{CAN} affected the neurons that set respiratory rhythm in the CRG in hamsters, but not in rats.

4.2.2. Respiratory burst amplitude is affected in rats more than hamsters by the elimination of both I_{NaP} and I_{CAN}

The elimination of only I_{NaP} by the application of riluzole resulted in a significant decrease in burst amplitude in hamsters at low concentrations of riluzole and in rats at higher concentrations (Figure 3-2B). I_{NaP} is important in promoting repetitive bursting in respiratory neurons (Crill, 1996; Del Negro *et al.*, 2002b). Blocking I_{NaP}, and therefore repetitive bursting, may impair the overall network ability to generate motor output and lead to an attenuation of the

amplitude of phrenic nerve discharges. Previous studies also show that application of riluzole reduced the amplitude of motor output from XII motor neurons (Del Negro *et al.*, 2005)(Del Negro *et al.*, 2002b). Riluzole decreased excitatory post-synaptic potentials and abolished repetitive firing (but not action potential generation) which had the net effect of reducing the excitability of XII motoneurons (Bellingham, 2006). The systemic application of riluzole in the present study would lead to similar effects on phrenic motor neurons and reduce neuronal excitability in the phrenic motor nucleus, accounting for our observed reduction in amplitude (Figure 3-2B).

Rat preparations, but not hamster preparations, significantly reduced amplitude in response to FFA concentrations ≤25 μM (Figure 3-5B). The fall in amplitude in rats likely was caused by the reduced excitability of the respiratory network that results from the elimination of I_{CAN} and all the other currents that FFA affects. Hamster preparations showed little response to FFA until higher concentrations. A response may have been observed if larger concentrations of FFA had been applied as was seen in weaned rats at concentrations >25 μM (Figure 3-7). Unfortunately, applying higher concentrations of FFA confound the interpretation of results due to the multiple effects of FFA at high doses (White & Aylwin, 1990; Farrugia *et al.*, 1993; Ottolia & Toro, 1994; Li *et al.*, 1998; Harks *et al.*, 2001; Stumpff *et al.*, 2001; Srinivas & Spray, 2003).

Coapplication of riluzole and FFA resulted in a significant decrease in amplitude in both hamster and rat preparations (Figure 3-9B). Similar to the frequency response, amplitude in hamsters was affected less by the coapplication of riluzole and FFA than by riluzole alone. Amplitude was reduced to 6% of baseline when riluzole was applied alone but only 55% when riluzole and FFA were coapplied (Figure 3-2B & Figure 3-9B), suggesting that FFA may mitigate the reduction in amplitude. Our results correspond with previous reports that show that coapplication of riluzole and FFA reduced or abolished burst amplitude in rats (Pena *et al.*, 2004; Del Negro *et al.*, 2005; Pace *et al.*, 2007b). Due to their functions in promoting repetitive bursting (I_{NaP}) and producing the inspiratory drive potential (I_{CAN}), eliminating I_{NaP} and I_{CAN} would lower the excitability of respiratory neurons (with or without intrinsic bursting properties) and impair the ability of the respiratory network to generate output to the respiratory motor neurons.

4.2.3. Hamster neural ventilation decreases more than rat upon elimination of both I_{NaP} and I_{CAN}

Eliminating I_{NaP} alone in hamster *in situ* preparations resulted in a significant decrease in neural ventilation ($n\dot{V}_E$) at lower concentrations than in rat preparations (Figure 3-2C). The decrease in $n\dot{V}_E$ in hamsters was produced by the decrease in both frequency and amplitude; in rats, the decrease in $n\dot{V}_E$ was caused by the decrease in amplitude. That respiratory rhythm generation in hamsters was very sensitive to elimination of I_{NaP} suggests that the hamster respiratory network may be configured differently than the network in rats or that I_{NaP} is more dominant among the mechanisms responsible for rhythm generation in hamsters. The low concentrations which elicited a change in frequency and the CVN validation recordings together suggest that this result is not a side effect of the non-specific actions of riluzole or instability of hamster *in situ* preparations.

Applying FFA resulted in a significant decrease in $n\dot{V}_E$ in rats while $n\dot{V}_E$ in hamster preparations remained around baseline values (Figure 3-5C). In both hamster and rats, any drop in $n\dot{V}_E$ due to FFA was caused by the observed decrease in amplitude (Figure 3-5B).

After applying riluzole and FFA to rat *in situ* preparations individually, concentrations of each drug were chosen for the coapplication of riluzole and FFA in order to give progressively larger inhibition of $n\dot{V}_E$. Applying these drug combinations resulted in significantly decreased $n\dot{V}_E$ in both hamster and rat preparations (Figure 3-9C). We calculated expected values for $n\dot{V}_E$ (Figure 3-10) on the assumption that the effect of the drugs would be additive. Comparing the expected values to the actual $n\dot{V}_E$ values obtained showed that, in the *in situ* preparation, $n\dot{V}_E$ declined more than was expected if the effects of riluzole and FFA were simply additive. This difference between expected and actual $n\dot{V}_E$ values also highlights the drastic difference between rats and hamsters to the elimination of I_{NaP} and I_{CAN}. More hamster preparations still exhibited fictive breathing following the elimination of I_{NaP} and I_{CAN}: only 30% of weaned rats but 86% of hamsters continued generating phrenic bursts at the highest concentration (Table 3-4). Hamsters decreased burst frequency more but defended amplitude better than rats, which decreased

amplitude more than frequency; however, both rats and hamsters suppressed $n\dot{V}_E$ to the same extent (Figure 3-9).

Considering the number of studies that have coapplied riluzole and FFA to rats and mice and observed little change in respiratory rhythm (Del Negro *et al.*, 2002b; Pena *et al.*, 2004; Del Negro *et al.*, 2005; Pace *et al.*, 2007b, a; Pena & Aguileta, 2007), the stark difference in the response to hamsters to elimination of I_{NaP} and I_{CAN} supports our hypothesis that hamsters are more reliant on these currents for rhythm generation, reflecting a fundamental difference in the CRG between rats and hamsters.

4.2.4. Increasing drive only rescues 'breathing' in rats

If the elimination of I_{NaP} and I_{CAN} reduces the excitability of the respiratory network and removes a source of drive to the CRG thereby decreasing $n\dot{V}_E$ in rat and hamster preparations, increasing the proportion of CO_2 in the perfusate of the *in situ* preparation to provide an alternate source of drive to the CRG should counteract the effect of the elimination of I_{NaP} or I_{CAN}. Increasing the proportion of CO_2 from 5% ($P_{CO2} \approx 42$ Torr) to 7% ($P_{CO2} \approx 52$ Torr) in the perfusate resulted in a large but not significant increase in the frequency of phrenic bursting in weaned rat preparations but no change in hamster preparations (Table 3-6). As riluzole and FFA were applied in hamsters, frequency values at 7% CO_2 tended to be greater, but not significantly, than values at 5% CO_2 (Figure 3-12C). In intact hamsters exposed to a 5% hypercapnic environment, frequency decreased, which does not correspond with our observed increase (Walker *et al.*, 1985). However, amplitude tended to be greater in 7% CO_2 preparations (Figure 3-13C) which agrees with the increase in amplitude seen in intact hypercapnic hamsters (Walker *et al.*, 1985). Overall ventilation increased in intact hamsters in response to hypercapnia (5%) while in the *in situ* preparation, $n\dot{V}_E$ was not different in 7% CO_2 preparations than in 5% CO_2 preparations (Figure 3-14C). In contrast, weaned rat preparations significantly increased $n\dot{V}_E$ (Figure 3-14C) in response to 7% CO_2 by increasing frequency (Figure 3-12C) and significantly increasing amplitude (Figure 3-13C). These results agree with previous studies in rat *in situ* preparations which reported that increasing perfusate P_{CO2} increased phrenic burst frequency (St.-John *et al.*, 2007) and increased amplitude resulting in an overall increase in neural ventilation

(Day & Wilson, 2005). Ventilation also increased in intact rats exposed to hypercapnia (Walker *et al.*, 1985)(Cragg & Drysdale, 1983).

In rats, providing an alternate source of drive to the CRG through activation of chemoreceptors recovered some of lost respiratory output due to application of riluzole and FFA, which is consistent with the primary effects of hypercapnia on amplitude. Increasing CO_2 in the hamster *in situ* preparations did not change total ventilation or the response to eliminating I_{NaP} and I_{CAN}; therefore, chemoreceptor drive to the respiratory network was not able to reduce the effects of eliminating I_{NaP} and I_{CAN}. These results suggest that increasing drive cannot replace the effects on rhythm that I_{NaP} and I_{CAN} provide. The estimated P_{CO2} of the 7% CO_2 is 52 Torr; *in vivo* hamster P_{CO2} is reported to be 52 Torr and does not change during exposure to a 5% hypercapnic environment (P_{CO2} = 55 Torr) (Walker *et al.*, 1985). Since hamsters have a blunted hypercapnic ventilatory response, the change in P_{CO2} in the perfusate may not have been enough to stimulate a chemosensory response in *in situ* hamster preparations; therefore, we cannot conclude if increasing drive is able to recover respiratory motor output in hamsters, as it does in rats.

4.3. Ontogenetic differences in I_{NaP} and I_{CAN}

A critical developmental window exists between 16 - 18 PND in rats where the ability to spontaneously recover from hypothermia-induced respiratory arrest is lost. We hypothesize that I_{NaP} and I_{CAN} are involved with initiating recovery and that reductions in the relative roles of I_{NaP} and I_{CAN} in the respiratory CRG result in this developmental transition.

4.3.1. Respiratory rhythm in young rats is more sensitive to application riluzole and FFA

Application of riluzole began reducing phrenic burst frequency in young rats significantly from baseline at 10 μM while phrenic burst frequency in weaned rat preparations remained at baseline levels (Figure 3-2A). This result is inconsistent with most published studies that report either that riluzole does not affect respiratory rhythm or that any effect that occurs is a result of riluzole blocking other currents in addition to I_{NaP} (Del Negro *et al.*, 2002b)(Del Negro *et al.*, 2005)(Paton *et al.*, 2006; Pena & Aguileta, 2007; St.-John *et al.*, 2007). One study reports that riluzole affects frequency in rats in a medullary *in situ* preparation (similar to the *in situ*

preparation but the pons is removed). However this data showed a decrease in amplitude only (not frequency) before motor output was abolished (Ramirez & Viemari, 2005). Based on the literature, which shows that I_{NaP} is eliminated by riluzole with EC_{50} = 3 μM in brainstem transverse slices, the change in frequency observed in the young rat preparations in the current study at 10 μM is most likely a result of the actions of riluzole on other channels in addition to blockade of I_{NaP} in young rats (Del Negro *et al.*, 2005). The decline in frequency occurred ≥10 μM riluzole in young rats leading to a significant difference between the two ages of rats suggesting that riluzole (all interactions) have more of an effect in young rats.

FFA application eliminated fictive breathing in young rat preparations as concentration increased so that only 60% of preparations remained active after the last concentration (Table 3-3). Applying FFA at a concentration of 25 μM had little effect on frequency and, therefore, respiratory rhythm generation in rats (Figure 3-5B). However, for rat preparations that did not continue to the last concentration of FFA (25 μM), respiratory rhythm was abolished due to amplitude reaching zero before frequency. Increasing FFA concentration to 100 μM resulted in a decrease in frequency however at this concentration the other multiple actions of FFA will be exerting non-specific effects on the expression of the respiratory rhythm (White & Aylwin, 1990; Farrugia *et al.*, 1993; Ottolia & Toro, 1994; Li *et al.*, 1998; Harks *et al.*, 2001; Stumpff *et al.*, 2001; Srinivas & Spray, 2003).

When riluzole and FFA are added in combination, no young rats continued bursting at the highest concentration (20 μM RIL + 15 μM FFA) whereas for both riluzole and FFA individually, young rat preparations continued generating bursts to the last concentration. The coapplication of riluzole and FFA also abolished phrenic motor output in all but 30% of weaned rat preparations (Table **3-4**) while all weaned rat preparations survived the individual applications of riluzole or FFA. Coapplication of riluzole and FFA during early post-natal development (in brainstem transverse slices) as well as at 9 - 13 PND (in *in vivo* mice) abolished respiratory rhythm, which corresponds to our data (Del Negro *et al.*, 2005; Pena & Aguileta, 2007). Phrenic burst frequency was affected in both ages of rats; however, the decrease in young rats was only significantly different from weaned rats at the highest concentration (>10 μM riluzole and 8 μM FFA) (Figure 3-9A), suggesting a developmental change occurs between 14 - 23 PND in the

sensitivity to riluzole and FFA in rats. Our data are consistent with the existence of a hypothesized developmental window where autoresuscitation ability is lost in non-hibernating species but the question of whether I_{NaP} and I_{CAN} mediate autoresuscitation requires direct testing.

4.3.2. Young rats are more dependent on I_{NaP} and I_{CAN} than weaned rats for producing motor output

Young rats significantly decreased amplitude at concentrations ≥12 μM riluzole while weaned rats maintained amplitude closer to baseline values resulting in a significant difference between the ages (Figure 3-2B). Riluzole is reported to reduce amplitude in rats and mice in *in situ* and brainstem transverse slice preparations suggesting that riluzole affects components of the respiratory network that are important for generating motor output (more than setting rhythm) (Pena *et al.*, 2004; Del Negro *et al.*, 2005; Ramirez & Viemari, 2005).

Both young and weaned rats decreased amplitude to the same extent during FFA application up to 25 μM (Figure 3-5B). In weaned rat preparations, applying FFA up to 100 μM reduced amplitude to zero in most preparations (Figure 3-7). I_{CAN} is responsible for the depolarization of the membrane of inspiratory neurons called the inspiratory drive potential, which facilitates neuronal bursting (Del Negro *et al.*, 2005)(Pena *et al.*, 2004; Pace *et al.*, 2007a). Therefore, attenuation of I_{CAN} would reduce the inspiratory drive potential and excitability of respiratory neurons, leading to decreased drive to the motor neurons and smaller amplitude. However, in brainstem transverse slice preparations, when inspiratory drive potential was eliminated by FFA, very little change was seen in the XII motor output (Pace *et al.*, 2007a); therefore, the observed decrease in motor output in the current study cannot only be attributed to attenuation of I_{CAN}. At doses between 25 - 100 μM, FFA will interfere with gap junctions and various Ca^{2+}, K^+ and Cl^- currents and have the overall affect of reducing excitability of the respiratory network (as discussed in section 4.1) (White & Aylwin, 1990; Farrugia *et al.*, 1993; Ottolia & Toro, 1994; Li *et al.*, 1998; Harks *et al.*, 2001; Stumpff *et al.*, 2001; Srinivas & Spray, 2003), which would also result in reducing amplitude.

Coapplication of riluzole and FFA significantly reduced amplitude in young and weaned rats similarly so that the age groups were not significantly different from each other (Figure 3-9B). Our results are supported by reports from rat and mouse brainstem transverse slice studies and

studies using intact awake mice which abolished inspiratory rhythm by coapplication of riluzole and FFA by mostly affecting the amplitude of the motor output (Pena & Aguileta, 2007)(Pena *et al.*, 2004; Del Negro *et al.*, 2005). With our systemic method of applying riluzole and FFA, the drugs would have access to all regions of the brain, so the change in motor output we saw likely were caused by the decreased neuronal excitability caused by the action of the drugs at multiple sites.

4.3.3. Ventilation in young rats declined more than in weaned rats

All our weaned rat preparations survived the elimination of I_{NaP} through the application of riluzole while the majority of young rat preparations did not (Table 3-3). $n\dot{V}_E$ was decreased more in young rats above 8 μM so the response of young rats was significantly different from the response of weaned rats (Figure 3-2C), suggesting that young rats are more sensitive to the elimination of I_{NaP} than weaned rats and may rely more on I_{NaP} for maintenance of rhythm generation.

Both rat groups significantly decreased $n\dot{V}_E$ after application of FFA (0.25 - 25 μM) so that no significant difference existed between the age groups (Figure 3-5C). When 25 - 100 μM FFA was applied to weaned rats, amplitude, frequency, and therefore $n\dot{V}_E$, all declined (Figure 3-7). Only one third of weaned rat preparations continued generating respiratory motor output past 50 μM FFA; the multiple effects of FFA at these concentrations could result in a decrease in frequency and/or amplitude of phrenic bursts due to reduced network excitability.

During coapplication of riluzole and FFA, $n\dot{V}_E$ decreased significantly in both age groups so that the groups were not significantly different (Figure 3-9C). The drop in $n\dot{V}_E$ was due to the decreases in both amplitude and frequency and was much greater than expected if the drugs had simply additive effects. Despite differences in the components, no significant difference in total $n\dot{V}_E$ existed between the age groups when I_{NaP} and I_{CAN} were eliminated together.

4.3.4. Increasing drive only rescues 'breathing' in weaned, not young, rats

Burst frequency (Figure 3-12A, B) increased in both weaned and young rats upon increasing the proportion of CO_2 from 5% to 7% in the perfusate. Amplitude (Figure 3-13A, B)

increased in 7% CO_2 more in weaned rats than in young rats. Therefore, neural ventilation (Figure 3-14A, B) increased in response to 7% CO_2 to a greater extent in weaned rats than in young rats. These results agree with observed hypercapnic ventilatory response in intact rats (Walker *et al.*, 1985)(Cragg & Drysdale, 1983) and rat *in situ* preparations (St.-John *et al.*, 2007) (Day & Wilson, 2005).

In weaned rats, $n\dot{V}_E$ was greater at 7% CO_2 than 5% CO_2, and it significantly dropped as drug concentrations increased but the significant difference between 7% CO_2 and 5% CO_2 preparations was maintained until the final concentration. In contrast, $n\dot{V}_E$ in young rats also increased in 7% CO_2 preparations but decreased significantly to match the values of 5% CO_2 preparations at higher drug concentrations. Hypercapnia seemed to ameliorate the effects of the drug combination on the amplitude in weaned rats; young rat burst amplitude decreased the same way in normal or high drive preparations. These results suggest that providing drive from chemoreceptors was able to reduce the degree to which amplitude and frequency were reduced but to different extents in young and weaned rats.

The lack of significant response from the young rats to the increase in CO_2 may to due to incomplete development of the hypercapnic ventilatory response. The hypercapnic ventilatory response in rats undergoes developmental changes in the first two weeks of life. In the first five days, response to hypercapnia is large and declines to a nadir at 8 PND. At 12 PND, ventilatory response just starts to increase from the nadir toward adult levels (Putnam *et al.*, 2005). Therefore at the ages used in the current study, the young rats (12 - 14 PND) are at their lowest level of responsiveness to CO_2 while the weaned rats have a fully developed hypercapnic ventilatory response.

Our results from weaned rats agree with brainstem transverse slice experiments where coapplication of RIL and FFA on rat and mouse slices abolished respiratory rhythm at 20 μM riluzole and 100 μM FFA (both at cellular and XII motor neuron activity) (Del Negro *et al.*, 2005). This effect was counteracted by increasing membrane excitability by application of substance P so the investigators concluded that I_{NaP} and I_{CAN} contribute to rhythm generation simply by increasing excitability and promoting inspiratory burst generation in all PBC neurons (Del Negro

et al., 2005). Our results confirm that riluzole and FFA reduce network excitability which can be rescued by substance P (Del Negro *et al.*, 2005) or increased chemoreceptor drive (Figure 3-14B).

4.4.Speculations

We observe that respiratory rhythm (frequency) in hamsters is more dependent on I_{NaP} than in rats. Our results from young rats also suggest that younger rats may be more dependent on I_{NaP} and I_{CAN} for rhythm generation than weaned rats. Although we do not test it directly here, our results are consistent with the 'hibernator as neonate' hypothesis. This hypothesis is derived from the observation that adult hibernators share a number of characteristics with neonates of all mammals (such as cold and hypoxia tolerance) (Harris *et al.*, 2004). In this case, reliance on I_{NaP} (and I_{CAN}) for rhythm generation may be a neonatal characteristic retained by hamsters into adulthood.

The ability to hibernate is not the only way in which hamsters and rats differ. Hamsters are fossorial species with well developed adaptations to living in hypoxic, hypercapnic burrows while rats are a more generalist species with fewer specific adaptations to fossorial lifestyles (Walker *et al.*, 1985; Frappell & Mortola, 1994). Non-pacemaker and I_{CAN}-mediated bursting neurons are proposed to be silent during hypoxia (Ramirez & Viemari, 2005). Therefore, living in chronic hypoxic burrows may have resulted in a reconfiguration of the hamster CRG to one that relies more on I_{NaP}-mediated bursting neurons (compared to the rat) since expression of I_{CAN} may have been reduced as hamsters adapted to their fossorial lifestyle. Our results that show that hamsters are very sensitive to riluzole application are consistent with a CRG that is more dependent on I_{NaP}-mediated mechanisms of rhythm generation. In addition, in hamsters P_{CO2} is greater and P_{O2} is less than that of rats at normoxia and normocapnia; therefore, central chemoreceptors may be active more in hamsters resulting in greater chemoreceptor drive to the PBC (Mulkey *et al.*, 2004). The increased tonic excitatory drive from central chemoreceptors could compensate for the lost source of drive from the reduced expression of I_{CAN}. Therefore, the reliance of hamsters of I_{NaP} for respiratory rhythm generation may stem from adaptations to a fossorial life.

4.5.Conclusions

Applying riluzole and FFA to *in situ* rat and hamster preparations resulted in a large decrease in the frequency of phrenic nerve bursting in hamsters in response to the elimination of I_{NaP}. Hamsters rely more on I_{NaP}-mediated mechanisms to set respiratory rhythm than rats. Therefore, a fundamental difference exists between adult rat and hamster respiratory rhythm generation. This species difference highlights the need to apply the models of rhythm generation based on rats and mice carefully across mammalian species.

When riluzole and FFA were applied to two age groups of rats, young rats (12 - 14 PND) tended to decrease frequency more than weaned rats (>23 PND); therefore, younger rats may be more reliant than weaned rats on I_{NaP} and I_{CAN}-mediated mechanisms of rhythm generation. Our data are consistent with the hypothesis that a developmental change occurs in the relative roles of I_{NaP} and I_{CAN} in the CRG of mammals.

Both hamsters and young rats showed a greater reliance on I_{NaP} and I_{CAN} for rhythm generation than weaned rats; both hamsters and young rats also can autoresuscitate. This correlation is consistent with the suggestion that I_{NaP} and I_{CAN}-mediated bursting neurons may facilitate recovery from hypothermic respiratory arrest.

5. References

Abdala, APL, Koizumi, H, St. John, WM, Moorgani, B, Smith, JC & Paton, JFR (2004). Role of persistent sodium current for generation of gasp- and eupneic respiratory activity in the *in situ* arterially perfused brainstem-spinal cord preparation. In *2004 Abstract Viewer/Itinerary Planner*, vol. Program No. 424.3. Society for Neuroscience, Washington, DC.

Adolph, EF (1951). Responses to hypothermia in several species of infant mammals. *Am J Physiol* **166,** 75-91.

Alzheimer, C, Schwindt, P & Crill, W (1993). Modal gating of Na+ channels as a mechanism of persistent Na+ current in pyramidal neurons from rat and cat sensorimotor cortex. *J Neurosci* **13,** 660-673.

Bellingham, MC (2006). Riluzole decreases synaptic excitation and repetitive firing in rat hypoglossal motor neurons. *2006 Neuroscience Meeting Planner Atlanta, GA Society for Neuroscience,* Program No. 237.235.

Benoit, E & Escande, D (1991). Riluzole specifically blocks inactivated Na channels in myelinated nerve fibre. *Pflugers Arch* **419,** 603-609.

Benoit, E & Escande, D (1993). Fast K-channels are more sensitive to riluzole than slow K-channels in myelinated nerve fibre. *Pflugers Arch* **422,** 536-538.

Butera Jr., RJ, Rinzel, J & Smith, JC (1999). Models of respiratory rhythm generation in the pre-Botzinger complex. I. Bursting pacemaker neurons. *J Neurophysiol* **81,** 382-397.

Cho, H, Kim, MS, Shim, WS, Yang, YD, Koo, J & Oh, U (2003). Calcium-activated cationic channel in rat sensory neurons. *Eur J Neurosci* **17,** 2630-2638.

Clancy, B, Darlington, RB & Finlay, BL (2001). Translating developmental time across mammalian species. *Neuroscience* **105,** 7-17.

Cragg, PA & Drysdale, DB (1983). Interaction of hypoxia and hypercapnia on ventilation, tidal volume and respiratory frequency in the anesthetized rat. *J Physiol* **341,** 477-493.

Crill, WE (1996). Persistent sodium current in mammalian central neurons. *Annu Rev Physiol* **58,** 349-362.

Darbon, P, Yvon, C, Legrand, J-C & Streit, J (2004). I_{NaP} underlies intrinsic spiking and rhythm generation in networks of cultured rat spinal cord neurons. *Eur J Neurosci* **20,** 976-988.

Day, TA & Wilson, RJA (2005). Specific carotid body chemostimulation is sufficient to elicit phrenic poststimulus frequency decline in a novel in situ dual-perfused rat preparation. *Am J Physiol* **289,** R532-544.

Del Negro, C, Morgado-Valle, C & Feldman, JL (2002a). Respiratory rhythm: an emergent network property. *Neuron* **34,** 821-830.

Del Negro, CA, Koshiya, N, Butera Jr., RJ & Smith, JC (2002b). Persistent sodium current, membrane properties and bursting behaviour of preBotzinger complex inspiratory neurons in vitro. *J Neurophysiol* **88,** 2242-2250.

Del Negro, CA, Morgado-Valle, C, Hayes, JA, Mackay, DD, Pace, RW, Crowder, EA & Feldman, JL (2005). Sodium and calcium current-mediated pacemaker neurons and respiratory rhythm generation. *J Neurosci* **25,** 446-453.

Doble, A (1996). The pharmacology and mechanism of action of riluzole. *Neurology* **47,** S233-S241.

Ellenberger, HH & Feldman, JL (1990). Subnuclear organization of the lateral tegmental field of the rat. I: Nucleus ambiguus and ventral respiratory group. *J Comp Neurol* **294,** 202-211.

Farrugia, G, Rae, JL, Sarr, MG & Szurszewski, JH (1993). Potassium current in circular smooth muscle of human jejunum activated by fenamates. *American Journal of Physiology Gastrointestinal and Liver Physiology* **265,** G873-879.

Faustino, EVS & Donnelly, DF (2006). An important functional role of persistent Na+ current in carotid body hypoxia transduction. *J Appl Physiol* **101,** 1076-1084.

Feldman, JL & Del Negro, CA (2006). Looking for inspiration: new perspectives on respiratory rhythm. *Nature Reviews Neuroscience* **7,** 232-241.

Frappell, PB & Mortola, JP (1994). Hamsters vs. rats: metabolic and ventilatory response to development in chronic hypoxia. *J Appl Physiol* **77,** 2748-2752.

Gogelein, H, Dahlem, D, Englert, HC & Lang, HJ (1990). Flufenamic acid, mefenamic acid and niflumic acid inhibit single nonselective cation channels in the rat exocrine pancreas. *FEBS Lett* **268,** 79-82.

Gray, PA, Janczewski, WA, Mellen, NM, McCrimmon, DR & Feldman, JL (2001). Normal breathing requires preBotzinger complex neurokinin-1 receptor-expressing neurons. *Nat Neurosci* **4,** 927-930.

Guinamard, R, Chatelier, A, Demion, M, Potreau, D, Patri, S, Rahmati, M & Bois, P (2004). Functional characterization of a Ca2+-activated non-selective cation channel in human atrial cardiomyocytes. *J Physiol* **558,** 75-83.

Hall, BJ & Delaney, KR (2002). Contribution of a calcium-activated non-specific conductance to NMDA receptor-mediated synaptic potentials in granule cells of the frog olfactory bulb. *J Physiol* **543,** 819-834.

Harks, EGA, de Roos, ADG, Peters, PHJ, de Haan, LH, Brouwer, A, Ypey, DL, van Zoelen, EJJ & Theuvenet, APR (2001). Fenamates: A novel class of reversible gap junction blockers. *J Pharmcol Exp Ther* **298,** 1033-1041.

Harris, MB, Olson, LE & Milsom, WK (2004). The origin of mammalian heterothermy: a case for perpetual youth? In *Life in the Cold: Evolution, Mechanisms, Adaptation, and Application. Twelfth International Hibernation Symposium*, vol. 27. ed. BARNES, B. M. & CAREY, H. V. Institute of Arctic Biology, University of Alaska, Fairbanks, Alaska, USA.

Hill, RW (2000). Anoxia tolerance to oxygen necessity: paradigm shift in the physiology of survival of apneic deep hypothermia in neonatal rodents. In *Life in the Cold.* ed. HELDMAIER, G. & KLINGENSPOR, M., pp. 199-205. Springer-Verlag, Heidelberg.

Johnson, SM, Koshiya, N & Smith, JC (2001). Isolation of the kernel for respiratory rhythm generation in a novel preparation: the pre-Botzinger complex "island". *J Neurophysiol* **85,** 1772-1776.

Johnson, SM, Smith, JC, Funk, GD & Feldman, JL (1994). Pacemaker behaviour of respiratory neurons in medullary slices from neonatal rat. *J Neurophysiol* **72,** 2598-2608.

Kochetkov, KV, Kazachenko, VN & Marinov, BS (2000). Dose-dependent potentiation and inhibition of single Ca^{2+}-activated K^+ channels by flufenamic acid. *Membr Cell Biol* **14,** 285-298.

Kononenko, NI, Shao, L-R & Dudek, FE (2004). Riluzole-sensitive slowly inactivating sodium current in rat suprachiasmatic nucleus neurons. *J Neurophysiol* **91,** 710-718.

Launay, P, Fleig, A, Perraud, A-L, Scharenberg, AM, Penner, R & Kinet, J-P (2002). TRPM4 is a Ca2+-activated nonselective cation channel mediating cell membrane depolarization. *Cell* **109,** 397-407.

Lee, RH & Heckman, CJ (2001). Essential role of a fast persistent inward current in action potential initiation and control of rhythmic firing. *J Neurophysiol* **85,** 472-475.

Li, L, Vapaatalo, H, Vaali, K, Paakkari, I & Kankaanranta, H (1998). Flufenamic and tolfenamic acids and lemakalim relax guinea-pig isolated trachea by different mechanisms. *Life Sci* **62,** PL303-PL308.

Liu, Q & Wong-Riley, MTT (2004). Developmental changes in the expression of GABAA receptor subunits $\alpha 1$, $\alpha 2$, and $\alpha 3$ in the rat pre-Botzinger complex. *J Appl Physiol* **96,** 1825-1831.

Marshall, LH (2005). Postnatal development of central rhythm generation of breathing in mammals. In *Zoology*, pp. 109. University of British Columbia, Vancouver.

McKay, LC, Janczewski, WA & Feldman, JL (2005). Sleep-disordered breathing after targeted ablation of preBotzinger complex neurons. *Nat Neurosci* **8,** 1142-1144.

Mellen, NM, Milsom, WK & Feldman, JL (2002). Hypothermia and recovery from respiratory arrest in a neonatal rat in vitro brain stem preparation. *Am J Physiol* **282,** R484-R491.

Mulkey, DK, Stornetta, RL, Weston, MC, Simmons, JR, Parker, A, Bayliss, DA & Guyenet, PG (2004). Respiratory control by ventral surface chemoreceptor neurons in rats. *Nat Neurosci* **7,** 1360-1369.

Ottolia, M & Toro, L (1994). Potentiation of large-conductance K-Ca channels by niflumic, flufenamic, and mefenamic Acids. *Biophys J* **67,** 2272-2279.

Pace, RW, Mackay, DD, Feldman, JL & Del Negro, CA (2007a). Inspiratory bursts in the preBotzinger complex depend on a calcium-activated non-specific cation current linked to glutamate receptors in neonatal mice. *J Physiol* **582,** 113-125.

Pace, RW, Mackay, DD, Feldman, JL & Del Negro, CA (2007b). Role of persistent sodium current in mouse preBotzinger Complex neurons and respiratory rhythm generation. *J Physiol* **580,** 485-496.

Partridge, LD, Muller, TH & Swandulla, D (1994). Calcium-activated non-selective channels in the nervous system. *Brain Res Brain Res Rev* **19,** 319-325.

Paton, JFR (1996). A working heart-brainstem preparation of the mouse. *J Neurosci Methods* **65,** 63-68.

Paton, JFR, Abdala, APL, Koizumi, H, Smith, JC & St-John, WM (2006). Respiratory rhythm generation during gasping depends on persistent sodium current. *Nat Neurosci* **9,** 311-313.

Paxinos, G & Watson, C (1986). *The rat brain in stereotaxic coordinates*. Academic Press Australia, Sydney.

Pena, F & Aguileta, M-A (2007). Effects of riluzole and flufenamic acid on eupnea and gasping of neonatal mice in vivo. *Neurosci Lett* **415,** 288-293.

Pena, F, Parkis, MA, Tryba, AK & Ramirez, J-M (2004). Differential contribution of pacemaker properties to the generation of respiratory rhythms during normoxia and hypoxia. *Neuron* **43,** 105-117.

Potts, JT, Spyer, KM & Paton, JFR (2000). Somatosympathetic reflex in a working heart-brainstem preparation of the rat. *Brain Res Bull* **53,** 59-67.

Ptak, K, Zummo, GG, Alheid, GF, Tkatch, T, Surmeier, DJ & McCrimmon, DR (2005). Sodium currents in medullary neurons isolated from the pre-Botzinger complex region. *J Neurosci* **25,** 5159-5170.

Putnam, RW, Conrad, SC, Gdovin, MJ, Erlichman, JS & Leiter, JC (2005). Neonatal maturation of the hypercapnic ventilatory response and central neural CO2 chemosensitivity. *Respir Physiol Neurobiol* **149,** 165-179.

Ramirez, J-M & Viemari, J-C (2005). Determinants of inspiratory activity. *Respir Physiol Neurobiol* **147,** 145-157.

Rekling, JC & Feldman, JL (1997). Calcium-dependent plateau potentials in rostral ambiguus neurons in the newborn mouse brain stem in vitro. *J Neurophysiol* **78,** 2483-2492.

Ren, J & Greer, JJ (2006). Modulation of respiratory rhythmogenesis by chloride-mediated conductances during the perinatal period. *J Neurosci* **26,** 3721-3730.

Richter, DW (1982). Generation and maintenance of the respiratory rhythm. *J Exp Biol* **100,** 93-107.

Richter, DW & Spyer, KM (2001). Studying rhythmogenesis of breathing: comparison of *in vivo* and *in vitro* models. *Trends Neurosci* **24,** 464-472.

Rybak, IA, Ptak, K, Shevtsova, NA & McCrimmon, DR (2003). Sodium currents in neurons from the rostroventrolateral medulla of the rat. *J Neurophysiol* **90,** 1635-1642.

Smith, JC, Butera Jr., RJ, Koshiya, N, Del Negro, C, Wilson, CG & Johnson, SM (2000). Respiratory rhythm generation in neonatal and adult mammals: the hybrid pacemaker-network model. *Respir Physiol* **122,** 131-147.

Smith, JC, Ellenberger, HH, Ballanyi, K, Richter, DW & Feldman, JL (1991). Pre-Botzinger complex: a brainstem region that may generate respiratory rhythm in mammals. *Science* **254,** 726-729.

Smith, JC, Koizumi, H, Abdala, APL & Paton, JFR (2004). The pre-Botzinger complex kernel for inspiratory rhythm and burst pattern generation: studies in the neonatal and adult rat *in situ* perfused brainstem-spinal cord. In *2004 Abstract Viewer/Itinerary Planner*, vol. Program No. 145.2. Society for Neuroscience, Washington, DC.

Solomon, IC, Chon, KH & Rodriguez, MN (2003). Blockade of brain stem gap junctions increases phrenic burst frequency and reduces phrenic burst synchronization in adult rat. *J Neurophysiol* **89,** 135-149.

Srinivas, M & Spray, DC (2003). Closure of gap junction channels by arylaminobenzoates. *Mol Pharmacol* **63,** 1389-1397.

St.-John, WM, Waki, H, Dutschmann, M & Paton, JFR (2007). Maintenance of eupnea of in situ and in vivo rats following riluzole: A blocker of persistent sodium channels. *Respir Physiol Neurobiol* **155,** 97-100.

Stumpff, F, Boxberger, M, Thieme, H, Strauβ, O & Wiederholt, M (2001). Flufenamic acid enhances current through maxi-K channels in the trabecular meshwork of the eye. *Current Eye Research* **22,** 427 - 437.

Tattersall, GJ & Milsom, WK (2003). Hypothermia-induced respiratory arrest and recovery in neonatal rats. *Respir Physiol Neurobiol* **137,** 29-40.

Thoby-Brisson, M & Ramirez, J-M (2001). Identification of two types of inspiratory pacemaker neurons in the isolated respiratory neural network of mice. *J Neurophysiol* **86,** 104-112.

Ueda, S & Ibuka, N (1995). An analysis of factors that induce hibernation in Syrian hamsters. *Physiol Behav* **58,** 653-657.

Urbani, A & Belluzzi, O (2000). Riluzole inhibits the persistent sodium current in mammalian CNS neurons. *Eur J Neurosci* **12,** 3567-3574.

Walker, BR, Adams, EM & Voelkel, NF (1985). Ventilatory responses of hamsters and rats to hypoxia and hypercapnia. *J Appl Physiol* **59,** 1955-1960.

Wenninger, JM, Pan, LG, Klum, L, Leekley, T, Bastastic, J, Hodges, MR, Feroah, TR, Davis, S & Forster, HV (2004). Large lesions in the pre-Botzinger complex area eliminate eupneic respiratory rhythm in awake goats. *J Appl Physiol* **97,** 1629-1636.

White, M & Aylwin, M (1990). Niflumic and flufenamic acids are potent reversible blockers of Ca2(+)- activated Cl- channels in Xenopus oocytes. *Mol Pharmacol* **37,** 720-724.

Wong-Riley, MTT & Liu, Q (2005). Neurochemical development of brain stem nuclei involved in the control of respiration. *Respir Physiol Neurobiol* **149,** 83-98.

6. Appendix

Table 6-1: T_I and T_E values for young rats, weaned rats and weaned hamsters in the riluzole trials. Asterisk (*) denotes significance from baseline.

[RIL] (μM)	T_I			T_E		
	Young rats	Weaned rats	Hamsters	Young rats	Weaned rats	Hamsters
0.0	1.00 ± 0.00	1.00 ± 0.00	1.00 ± 0.00	1.00 ± 0.00	1.00 ± 0.00	1.00 ± 0.00
0.2	1.04 ± 0.02	0.98 ± 0.02	1.12 ± 0.06	1.02 ± 0.02	1.07 ± 0.02	1.38 ± 0.18
1.0	0.93 ± 0.02	0.96 ± 0.02	1.19 ± 0.07	1.07 ± 0.06	1.07 ± 0.04	1.50 ± 0.23
2.0	0.88 ± 0.01	0.97 ± 0.04	1.18 ± 0.16	1.06 ± 0.08	1.09 ± 0.06	1.89 ± 0.31
4.0	0.94 ± 0.03	0.84 ± 0.04	1.15 ± 0.08	1.27 ± 0.21	1.09 ± 0.08	2.04 ± 0.46
6.0	0.92 ± 0.06	0.83 ± 0.05	1.10 ± 0.13	1.75 ± 0.40	1.15 ± 0.11	2.94 ± 0.45
8.0	0.92 ± 0.08	0.94 ± 0.07	1.29 ± 0.17	2.16 ± 0.62	1.09 ± 0.15	2.98 ± 1.81
10.0	1.02 ± 0.17	1.04 ± 0.08	1.05 ± 0.22	2.57 ± 0.74	1.19 ± 0.22	2.66 ± 0.63
12.0	1.11 ± 0.31	1.15 ± 0.10	1.55	3.31 ± 1.85	1.30 ± 0.27	5.25
14.0	1.46 ± 0.67	1.20 ± 0.09	1.42	1.58 ± 0.33	1.32 ± 0.26	7.15
16.0	1.46 ± 0.70	1.21 ± 0.14		1.91 ± 0.30	1.43 ± 0.28	
18.0	1.51 ± 0.71	1.30 ± 0.12		2.84 ± 0.63	1.65 ± 0.41	
20.0	1.30 ± 0.37	1.32 ± 0.12		4.48 ± 2.06*	1.72 ± 0.32	

Table 6-2: T_I and T_E values for young rats, weaned rats and weaned hamsters in the FFA trials.

[FFA] (μM)	T_I			T_E		
	Young rats	Weaned rats	Hamsters	Young rats	Weaned rats	Hamsters
0.00	1.00 ± 0.00	1.00 ± 0.00	1.00 ± 0.00	1.00 ± 0.00	1.00 ± 0.00	1.00 ± 0.00
0.25	1.10 ± 0.16	1.05 ± 0.05	0.97 ± 0.03	1.04 ± 0.07	0.99 ± 0.11	1.01 ± 0.07
1.25	0.98 ± 0.05	1.02 ± 0.01	1.07 ± 0.07	0.98 ± 0.07	0.95 ± 0.08	0.97 ± 0.05
2.50	0.87 ± 0.05	0.95 ± 0.03	0.97 ± 0.08	1.00 ± 0.06	0.97 ± 0.14	0.91 ± 0.09
5.00	0.81 ± 0.07	1.03 ± 0.04	0.89 ± 0.12	1.02 ±0.08	0.95 ± 0.12	0.87 ± 0.10
7.50	0.81 ± 0.06	1.08 ± 0.09	0.87 ± 0.11	1.34 ± 0.34	0.92 ± 0.10	0.88 ± 0.12
10.00	0.70 ± 0.03	1.19 ± 0.22	0.62 ± 0.06	0.80 ± 0.12	0.99 ± 0.13	0.87 ± 0.10
12.50	0.73 ± 0.02	1.24 ± 0.29	0.72 ± 0.06	0.89 ± 0.20	1.29 ± 0.39	0.96 ± 0.15
15.00	0.63 ± 0.01	1.24 ± 0.33	0.92 ± 0.08	1.23 ± 0.68	1.04 ± 0.09	0.90 ± 0.14
17.50	0.61 ± 0.03	1.02 ± 0.13	0.87 ± 0.10	0.52 ± 0.04	1.47 ± 0.42	0.75 ± 0.10
20.00	0.64 ± 0.04	1.03 ± 0.14	0.88 ± 0.09	0.51 ± 0.04	1.11 ± 0.11	0.91 ± 0.22
22.50	0.64 ± 0.03	0.91 ± 0.09	0.78 ± 0.16	0.37 ± 0.03	1.81 ± 0.63	0.76 ± 0.18
25.00	0.63 ± 0.04	0.83 ± 0.15	0.66 ± 0.16	0.35 ± 0.03	2.12 ± 1.23	1.00 ± 0.32

Table 6-3: T_I and T_E data for young rats, weaned rats and weaned hamsters in the trials with coapplication of riluzole and FFA.

[RIL]/[FFA]	T_I			T_E		
	Young rats	Weaned rats	Hamsters	Young rats	Weaned rats	Hamsters
0 μM	1.00 ± 0.00	1.00 ± 0.00	1.00 ± 0.00	1.00 ± 0.00	1.00 ± 0.00	1.00 ± 0.00
6μM/2.5μM	0.89 ± 0.03	0.84 ± 0.02	1.11 ± 0.12	1.34 ± 0.11	1.03 ± 0.08	1.85 ± 0.35
7.5μM/5μM	0.92 ± 0.02	0.81 ± 0.02	1.19 ± 0.19	1.54 ± 0.16	1.11 ± 0.09	3.37 ± 0.75
9μM/6μM	1.04 ± 0.06	0.99 ± 0.06	1.24 ± 0.19	2.14 ± 0.33	1.32 ± 0.18	15.46 ± 6.32
10μM/8μM	1.15 ± 0.09	1.01 ± 0.07	1.26 ± 0.26	2.33 ± 0.38	1.52 ± 0.23	37.42 ± 25.8
12μM/10μM	1.09 ± 0.09	1.12 ± 0.05	0.99 ± 0.24	2.62 ± 0.75	2.09 ± 0.56	28.30 ± 17.8
20μM/15μM		1.30 ± 0.30	1.33 ± 0.27		3.56 ± 1.02	3.25 ± 0.96

Table 6-4: T_I and T_E values for young rats, weaned rats and weaned hamsters in the trials with coapplication of riluzole and FFA

[RIL]/[FFA]	T_I			T_E		
	Young rats	Weaned rats	Hamsters	Young rats	Weaned rats	Hamsters
0 μM	1.10 ± 0.08	0.93 ± 0.07	1.01 ± 0.19	1.16 ± 0.07	1.29 ± 0.23	0.94 ± 0.22
6μM/2.5μM	1.07 ± 0.09	0.92 ± 0.06	1.12 ± 0.22	1.28 ± 0.18	1.59 ± 0.47	2.10 ± 0.66
7.5μM/5μM	1.28 ± 0.07	1.06 ± 0.10	1.90 ± 0.85	1.95 ± 0.52	1.72 ± 0.55	4.06 ± 2.24
9μM/6μM	1.17 ± 0.08	1.11 ± 0.11	3.01 ± 1.62	1.31 ± 0.13	1.80 ± 0.56	5.64 ± 3.30
10μM/8μM	1.21 ± 0.09	1.10 ± 0.14	5.26 ± 2.76	1.48 ± 0.18	2.06 ± 0.71	17.27 ± 14.89
12μM/10μM	1.25 ± 0.13	1.21 ± 0.16	4.34 ± 2.16	2.04 ± 0.32	2.17 ± 0.74	6.44 ± 5.03
20μM/15μM	1.18 ± 0.14	1.13 ± 0.17	1.47 ± 0.39	5.38 ± 4.56	3.44 ± 1.00	4.19 ± 1.31